Journal of Human Evolution 219 (2026) 103887

Contents lists available at ScienceDirect

Journal of Human Evolution

journal homepage: www.elsevier.com/locate/jhevol

Neanderthal's heel: How the Neanderthal's external calcaneal shape uniquely differs from that of modern humans

Rita Sorrentino [a, b, *], Silvia Volpe [b], Kristian J. Carlson [c, d], Teresa Nicolosi [b, e], Carla Figus [e], Vitale Sparacello [f], Francesca Meli [a], Michele Conconi [g], Nicola Sancisi [g], Claudio Belvedere [h], Alberto Leardini [h], Jean-Jacques Hublin [i, j], Timothy Ryan [k], Luca Sineo [a], Antonio Rosas [l], Stefano Benazzi [e, m], Maria Giovanna Belcastro [b]

[a] Department of Biological, Chemical and Pharmaceutical Sciences and Technologies (STEBICEF), University of Palermo, Palermo, 90123, Italy
[b] Department of Biological, Geological and Environmental Sciences, University of Bologna, Bologna, 40126, Italy
[c] Division of Integrative Anatomical Sciences, Keck School of Medicine, University of Southern California, Los Angeles, 90033, USA
[d] Evolutionary Studies Institute, University of the Witwatersrand, Johannesburg, WITS 2050, South Africa
[e] Department of Cultural Heritage, University of Bologna, Ravenna, 48121, Italy
[f] Department of Life and Environmental Sciences, University of Cagliari, Cittadella Monserrato, Cagliari, 09124, Italy
[g] Department of Industrial Engineering, Health Sciences and Technologies, Interdepartmental Centre for Industrial Research (HST–ICIR), University of Bologna, Bologna, 40136, Italy
[h] Laboratory of Movement Analysis and Functional Evaluation of Prostheses, IRCCS Istituto Ortopedico Rizzoli, Bologna, 40136, Italy
[i] Chaire Internationale de Paléoanthropologie, CIRB (UMR 7241–U1050), Collège de France, Paris, 75005, France
[j] Max Planck Institute for Evolutionary Anthropology, Leipzig, 04103, Germany
[k] Department of Anthropology, The Pennsylvania State University, State College, PA, 16802, USA
[l] Group of Paleoanthropology, Department of Palaeobiology, Museo Nacional de Ciencias Naturales (CSIC), Madrid, 28006, Spain
[m] Department of Archaeology, Samarkand State University named after Sharof Rashidov, Boulevard 15, Samarkand, 140129, Uzbekistan

ARTICLE INFO

Article history:
Received 20 October 2025
Accepted 25 July 2026
Available online xxx

Keywords:
Foot
Functional morphology
Longitudinal arch
Geometric morphometrics
Locomotion

ABSTRACT

Neanderthals exhibit unique morphological adaptations in their calcaneus compared to *Homo sapiens*, shedding light on distinct evolutionary pressures and functional requirements shaping their respective foot anatomy. This study assesses which calcaneal traits represent plesiomorphic, autapomorphic, and/or functional adaptations. Geometric morphometrics was used to analyze the external shape of 7 Neanderthal and 64 *H. sapiens* calcanei spanning early Upper Pleistocene hunter-gatherers to post-industrial populations. Shape, size, and allometric differences were assessed among groups, enabling detailed examination of the whole calcaneus and key subregions such as talar facets, the cuboid facet, and the tuberosity. Compared to calcanei of *H. sapiens*, calcanei of Neanderthals were shorter, wider, and taller—distinct adaptations likely favoring more load-bearing over the rearfoot and high mobility. Similar but less pronounced traits appear in highly mobile, unshod modern humans, while sedentary, postindustrial populations show more gracile calcanei, likely influenced by footwear and reduced activity. Neanderthals also displayed ancestral features such as a shorter sinus tarsi. Notably, Neanderthal subtalar joint shape and calcaneocuboid orientation suggest a habitually pronated foot posture. Neanderthals also exhibit a reduced lateral plantar process compared to *H. sapiens*, implicating differences in plantar ligament attachment and foot arch support. Differences in the cuboid facet and tuberosity of Neanderthals and *H. sapiens* imply alternative strategies for foot stabilization and force transmission through proximal tarsal joints, likely reflecting a different longitudinal arch expression, one adapted to Neanderthals' body mass and high-activity lifestyle.

1. Introduction

The human ankle and foot bones have significantly advanced our understanding of the behavioral adaptations across primates

* Corresponding author.
E-mail address: rita.sorrentino01@unipa.it (R. Sorrentino).

https://doi.org/10.1016/j.jhevol.2026.103887

including hominins (Harcourt-Smith and Aiello, 2004; Holowka and Lieberman, 2018; McNutt et al., 2018; DeSilva et al., 2019). Functional adaptation of the human skeleton to bipedalism has focused on external shape of the ankle and foot bones (Latimer et al., 1987; Fernández et al., 2018; Sorrentino et al., 2020a, 2023; Harper et al., 2021; Nozaki et al., 2021; Marchi et al., 2022; Harper, 2023; Dann et al., 2024; Pietrobelli et al., 2024a; Tomizawa et al., 2024), their trabecular bone remodeling (DeSilva and Devlin, 2012; Zeininger et al., 2016; Su and Carlson, 2017; Tsegai et al., 2017, 2018; Saers et al., 2018; DeMars et al., 2020; Koneru and Harper, 2024), and foot kinematics (Griffin et al., 2010; Greiner and Ball, 2014; Holowka et al., 2017; Finestone et al., 2018; O'Neill et al., 2018).

Among the tarsal bones, the calcaneus, having a crucial role in weight-bearing and force transmission at heel strike during bipedal locomotion, has undergone significant changes throughout human evolution (Webber and Raichlen, 2016; Zeininger et al., 2020; Harper et al., 2021, 2022b; Prang, 2024). Thanks to its central role in promoting a mechanically efficient bipedal gait, the calcaneus is particularly well suited for exploring the link between form and function.

Anatomically, the calcaneus articulates superiorly with the talus through the posterior and anterior talar facets and distally with the cuboid. Compared to those of great apes, the human calcaneus exhibits unique features associated with bipedalism such as a larger tuberosity providing a strong attachment for the Achilles tendon and lever arm for the triceps surae, both being adaptive for forward propulsion, and a flatter posterior talar facet to reduce subtalar joint mobility (Latimer and Lovejoy, 1989; Prang, 2015a, 2016). A more plantarly oriented lateral plantar process of the calcaneus in *Homo sapiens* purportedly provides additional support and stability during weight-bearing activities (Boyle et al., 2018; Harper et al., 2021). In comparison, the more concave cuboid articular surface and projecting peroneal trochlea typical of ape calcanei have been associated with increased subtalar joint mobility (i.e., inversion and eversion) that is adaptive for climbing (Gebo, 1992; Gebo and Schwartz, 2006; Harper et al., 2021; Nozaki et al., 2021). These morphological adaptations reflect evolutionary pressures that have shaped calcaneal anatomy to optimize performance during the respective behavioral patterns.

Although the precise point at which modern human–like calcaneal morphology emerged in our evolutionary lineage remains uncertain, the prevailing hypothesis is that *Australopithecus afarensis* exhibits more humanlike characteristics than other *Australopithecus* species, *Homo habilis*, or *Paranthropus boisei* (Zipfel et al., 2011; Prang, 2015b; Boyle et al., 2018; McNutt et al., 2018; Harper et al., 2021). While there is a gap in the fossil record of early *Homo* calcanei, both in Africa and Eurasia, Middle and Upper Pleistocene *Homo* taxa both in Africa and Eurasia are represented in the fossil record (Pablos, 2015; DeSilva et al., 2019). Specifically, Middle Pleistocene calcanei have been recovered from *Homo naledi* (from 236 to 335 kyr) who still retain some apelike traits (Harcourt-Smith et al., 2015; Harper et al., 2021). In contrast, calcanei from Sima de los Huesos (~430 kyr; Atapuerca Mountains, Spain) and *Homo neanderthalensis* (~300–40 kyr) in Eurasia, as well as those from Jinniushan (~260 kyr; China), are generally more similar to those of anatomically modern humans, despite some features indicating functional or phylogenetic divergence from *H. sapiens* (Trinkaus, 1983; Lu et al., 2011; Pablos et al., 2014; Pablos, 2015; Pablos and Arsuaga, 2024).

Particularly, *H. neanderthalensis* (hereafter called Neanderthals) and *H. sapiens* share anatomical pedal features, as well as exhibit significant differences (Harvati, 2010). Neanderthal foot bones purportedly reflect their overall postcranial musculoskeletal robusticity, as indicated by thicker and larger bones, more curved femora, and strongly marked muscle insertions particularly in the lower limbs (Trinkaus et al., 1991; Pearson, 2000; De Groote, 2011; Belcastro et al., 2020). Although Neanderthal foot bones are almost indistinguishable from those of modern humans, Neanderthals exhibit larger joint surfaces and more robust tarsals and metatarsals that suggest higher biomechanical loadings due to higher activity levels and greater body mass (Trinkaus, 1983; Trinkaus et al., 1991; Pablos et al., 2014, 2017; Pearson et al., 2020; Sorrentino et al., 2021). Neanderthal generalized lower limb robusticity is extended to the calcaneus, given its role in weight transfer, in the form of large talar facets, a projecting sustentaculum tali, and a mediolaterally wide tuberosity (Trinkaus, 1983; Pablos et al., 2014). These Neanderthal traits are shared by calcanei from Sima de los Huesos, possibly suggesting a phylogenetic relationship of these two paleodemes and perhaps likely indicating a similarly large body size in both (Pablos and Arsuaga, 2024). While there is no doubt about obligate terrestrial bipedality in Neanderthals, their running performance capabilities are debatable (Raichlen et al., 2011). Distinguishing which traits are more functionally related or represent derived features of Neanderthals requires careful consideration of the variables, both environmental and cultural, influencing their foot morphology. In this study, we contribute to this research topic by using geometric morphometrics to examine external shape of the calcaneus in Neanderthals compared to various groups of *H. sapiens* with different mobility strategies.

Factors used to frame the morphological differences between Neanderthals and *H. sapiens* are primarily mobility levels, accounting for the distances regularly traveled due to shifts in subsistence strategies (e.g., within *H. sapiens* this includes mobile hunter-gatherers → sedentary agriculturalists → high sedentary postindustrial societies). Several studies have indicated that reduced physical activity and mobility levels have driven skeletal gracilization in *H. sapiens* from the Pleistocene to the Holocene (Carlson and Marchi, 2014; Chirchir et al., 2015; Ryan and Shaw, 2015). This affects many regions of the body and has been well studied in foot bones (Saers et al., 2018; DeMars et al., 2020; Sorrentino et al., 2020b, 2021; Harper, 2023; Dann et al., 2024). Studies on bone robusticity and estimates of energetic expenditure for foraging, as well as associated technocomplexes and prevailing climatic conditions, suggest that Neanderthals and Middle Pleistocene/early Upper Pleistocene (EUP) *H. sapiens* were characterized by high mobility, exceeding that of *H. sapiens* hunter-gatherers from the late Upper Pleistocene (LUP) (Holt, 2003; Weaver and Steudel-numbers, 2005; Holt and Formicola, 2008; Shaw and Stock, 2011). Thus, our expectation is that if certain traits of the Neanderthal calcaneus reflect high mechanical stress due to elevated levels of mobility, these traits should also be present in EUP *H. sapiens* specimens in our sample (i.e., Qafzeh and Skhul) but presumably to a lesser degree in LUP individuals that are closer to modernity. However, if there are calcaneal features shared between Neanderthals and early *H. sapiens*, then these may represent ancestral retentions. Therefore, empirical comparisons with Middle Pleistocene *Homo* fossils from Sima de los Huesos (Pablos et al., 2014, 2017; Pablos and Arsuaga, 2024) and Jinniushan (Lu et al., 2011) should be helpful to attempt to discern whether any of these traits are the result of either ancestry or high levels of behaviorally driven mechanical stress.

Additionally, footwear use, spanning from prehistoric functional protection to modern industrialized designs, has profoundly influenced bone structure (Trinkaus, 2005; Carlson et al., 2007; Zipfel and Berger, 2007; Willems et al., 2017). Early footwear, emerging in the LUP, reduced mechanical loading on foot bones, leading to decreased robustness of bones and increased incidence

of pathologies (e.g., hallux valgus, metatarsal deformities). Industrialization exacerbated these trends by introducing sedentary lifestyles (Trinkaus, 2005; Hatala et al., 2013; Willems et al., 2017; Holowka et al., 2018, 2022; Wallace et al., 2018; Sorrentino et al., 2020b). In this context, evidence from footprints suggests that Neanderthals in Europe, and even LUP *H. sapiens* populations, walked without footwear (Lockley et al., 2008; Citton et al., 2017; Duveau et al., 2019; Muñiz et al., 2019; Bennett et al., 2021; Neto de Carvalho et al., 2025). We expect to recognize certain calcaneal traits that may be correlated with unshod walking or walking with soft foot coverings among Neanderthals and *H. sapiens* hunter-gatherers, compared to the hard-soled shoes used by post-industrial *H. sapiens* groups. Indeed, studies have shown that heel strike patterns change in barefoot populations. For instance, barefoot walking tends to involve a more midfoot or forefoot strike, which reduces heel impact forces compared to those during shod walking (Lieberman, 2014; Holowka et al., 2018; Wallace et al., 2018). Additionally, barefoot walking often involves greater ankle compliance in multiple planes (Wallace et al., 2018), while footwear increases ankle dorsiflexion (López et al., 2023). Thus, differences in foot bone morphology distinguish populations with varying footwear habits (Trinkaus, 2005; Saers et al., 2018; Sorrentino et al., 2020b, 2021; Harper, 2023; Dann et al., 2024).

Finally, it has been suggested that Neanderthal tali reveal some autapomorphic traits in the subtalar joint that indicate a predisposition for pronated foot posture. This unique morphology is thought to reflect a plastic response to greater body mass and/or mechanical stress (Sorrentino et al., 2021). Here, we hypothesize that talar facets of the calcaneus will mirror these derived features in the articulating surfaces of the talus, which would confirm a unique foot posture in Neanderthals.

This study will further elucidate ancestral, derived, and plastic features that reflect variability in locomotor adaptations, thereby enhancing our understanding of Neanderthal foot anatomy.

2. Materials and methods

2.1. Sample

The sample consists of 71 three-dimensional (3D) digital models of calcanei of adult individuals (7 Neanderthals and 64 *H. sapiens*; Table 1), without evident signs of pathologies. In the majority of cases, left calcanei were used, but when unavailable, the right calcaneus was mirrored for inclusion in geometric morphometric analyses.

The Neanderthal calcanei in this study include late (classical) Neanderthals: Regourdou 1, La Chapelle, La Ferrassie 1 and 2, El Sidrón SD-2192 and SDR-112, and Spy 2.

Regourdou 1 is a young adult of indeterminate sex retrieved at the Regourdou site (Montignac, France). The individual has been dated to 70–56 ka BP (Bonifay, 1964; Pablos et al., 2019). La Chapelle is from a male individual found in La Bouffia Bonneval cave at La Chapelle-aux-Saints (France), dated to 56–47 ka BP, and is now stored at the Muséum National d'Histoire Naturelle, Département Hommes, Natures, Sociétés, in Paris, France (Grün and Stringer, 1991). At the Mousterian site of La Ferrassie (France), two skeletons were found, known as La Ferrassie 1 and 2, dated to 54–40 ka BP (Heim, 1976, 1982; Guérin et al., 2015). La Ferrassie 1 was a male Neanderthal, while La Ferrassie 2 was a female (Gómez-Olivencia et al., 2018). From El Sidrón (Asturias, Spain) two calcanei have been analyzed, SD-2192 and SDR-112, for which the sex is indeterminate due to the fragmentary nature of

Table 1
Sample of *Homo sapiens* and *Homo neanderthalensis* for this study.

Sample	Time period	Geographical location	Subsistence
Neanderthals ($n = 7$)			
Regourdou 1	70–56 ka BP	France	Hunter-gatherer
La Chapelle	56–47 ka BP	France	Hunter-gatherer
La Ferrassie 1	54–40 ka BP	France	Hunter-gatherer
La Ferrassie 2	54–40 ka BP	France	Hunter-gatherer
El Sidrón (SD-2192)	49 ka BP	Spain	Hunter-gatherer
El Sidrón (SDR-112)	49 ka BP	Spain	Hunter-gatherer
Spy 2	36 ka BP	Belgium	Hunter-gatherer
Homo sapiens			
Early Upper Pleistocene ($n = 3$)			
Qafzeh 8	120–90 ka BP	Israel	Hunter-gatherer
Qafzeh 9	120–90 ka BP	Israel	Hunter-gatherer
Skhul 4	120–90 ka BP	Israel	Hunter-gatherer
Late Upper Pleistocene ($n = 7$)			
Dolní Věstonice 15	~31 ka cal. BP	Czech Republic	Hunter-gatherer
San Teodoro 1	15–14 ka cal. BP	Italy	Hunter-gatherer
Arene Candide 2	13–12 ka cal. BP	Italy	Hunter-gatherer
Arene Candide 3	13–12 ka cal. BP	Italy	Hunter-gatherer
Arene Candide 5	13–12 ka cal. BP	Italy	Hunter-gatherer
Arene Candide 10	13–12 ka cal. BP	Italy	Hunter-gatherer
Arene Candide 14	13–12 ka cal. BP	Italy	Hunter-gatherer
Iron age group ($n = 8$)			
Baucina	7th–5th c. BCE[a]	Italy	Farmers/foragers
Postindustrial group ($n = 46$)			
Bologna	19th–20th c. CE[b]	Italy	Urban laborers and specializations

[a] Chronology estimated based on contextual and archaeological data.
[b] Chronology based on cemetery record.

both individuals. They have been dated to 49 ka BP (Rosas et al., 2006; Wood et al., 2013). Spy 2 is an individual found in Spy Cave (Belgium), for which the sex cannot yet be reliably determined as studies report conflicting results (Holloway et al., 2005; Chapman et al., 2013). This individual has been dated to 36 ka BP, making it one of the most recent Neanderthals in Europe prior to their extinction (Semal et al., 2009).

The *H. sapiens* sample includes early and LUP hunter-gatherers, Iron Age farmers/foragers, and a postindustrial group.

The EUP group includes Qafzeh and Skhul individuals (Israel) dated to 120–90 ka BP. Skhul 4 is located at the Rockefeller Museum of Jerusalem (Israel), and he was a 40-year old male discovered in a cave near Mount Carmel (Mount Mar Elias) from the Upper Galilee. Qafzeh 8 and 9 are from Qafzeh cave (Israel) and are curated at Tel Aviv University (Israel). The Qafzeh 9 individual is originally assessed as an adult female (Vandermeersch, 1981; but see Castejón-Molina and Pablos, 2021; Coutinho-Nogueira et al., 2021) from the most ancient double burial discovered to date, whereas Qafzeh 8 was initially described as male by Vandermeersch (1981), but this identification was later not confirmed (Vandermeersch and Bar-Yosef, 2019). The EUP sample represents a hunter-gatherer *H. sapiens* group with presumably higher mobility than other *H. sapiens* groups in the study, as suggested by anatomical and archaeological data reconstructing EUP locomotor behaviors (Holt, 2003; Weaver and Steudel-numbers, 2005; Holt and Formicola, 2008; Shaw and Stock, 2011). Based on chronology, shared ancestral characteristics of the calcaneus are expected to be more prevalent in Neanderthals and Early Upper Paleolithic *H. sapiens* than in either of these groups when compared to all more recent *H. sapiens* groups.

The LUP group includes Dolní Věstonice 15 (Czech Republic), San Teodoro 1 (Italy), and five calcanei from Arene Candide (Italy). The calcaneus of Dolní Věstonice 15 belonged to a Gravettian male individual from the eponymous site from the Czech Republic dated to ~31 ka cal. BP (Formicola et al., 2001; Fewlass et al., 2019). Calcanei from Arene Candide originate from late Epigravettian burials in the eponymous cave in Finale Ligure, Liguria (Italy) dated to 13–12 ka cal. BP (Sparacello et al., 2018a, 2021). Another late Epigravettian individual is San Teodoro 1 from Grotta di San Teodoro near Acquedolci (province of Messina, Italy) dated to 15,315–14,255 and 15,232–14,126 ka cal. BP (Sineo et al., 2002; D'Amore et al., 2009; Forgia et al., 2025) and stored at the Museo di Paleontologia G.G. Gemellaro in Palermo (Italy). The LUP group represents a *H. sapiens* population whose subsistence was based on hunting and foraging. Their lifestyle involved high levels of physical activity and mobility, although these levels were likely less intense than those of EUP hunter-gatherers (Holt, 2003; Trinkaus, 2005; D'Amore et al., 2009; Sparacello et al., 2018b; Pietrobelli et al., 2024b).

The Iron Age group from Baucina ($n = 8$, undetermined sex) originated from the archaeological site of Monte Falcone in Sicily, Italy, inhabited by Sikans, an indigenous group of Sicily. Archaeological findings at this site indicate subsistence practices such as cereal farming, animal domestication, and foraging, which likely contributed to increased sedentarization in this group during the period from 7th to 5th c. BCE (Belvedere et al., 2016). Lastly, the postindustrial group ($n = 46$, including 24 males and 22 females) originates from the Documented Human Osteological Collection (DHOC) of the Certosa Cemetery of Bologna (Italy) (19th–20th c. CE). It represents the most sedentary group within this study, characterized by individuals who habitually wore heavy shoes and boots during their occupational activities in the city of Bologna (Belcastro et al., 2017; Sorrentino et al., 2020b, 2022, 2025).

2.2. Digital data collection

The 3D surface reconstructions were acquired by laser scanning, CT, or μCT scans of the original specimens. These techniques have been shown to give comparable results (Brzobohatá et al., 2012; Sorrentino et al., 2021; Pietrobelli et al., 2022). In the case of CT or μCT scans, Avizo v. 9.2 (Thermo Fisher Scientific, Waltham) was used to generate 3D digital models (isosurface reconstructions) from the image data.

A 3D model of the Regourdou 1 calcaneus was obtained from μCT scanning (voxel resolution of 0.0455 × 0.0455 × 0.0457 mm) conducted at the European Synchrotron Radiation Facility in Grenoble, France. Structured light scanning of the calcaneal surface of La Chapelle, as well as CT scans of calcanei of La Ferrassie 1 (voxel size: 0.219 × 0.219 × 0.400 mm) and La Ferrassie 2 (voxel size = 0.251 × 0.251 × 0.500 mm) were kindly provided by the Muséum National d'Histoire Naturelle, Département Hommes, Natures, Sociétés (Paris, France). The 3D models of SD-2192 and

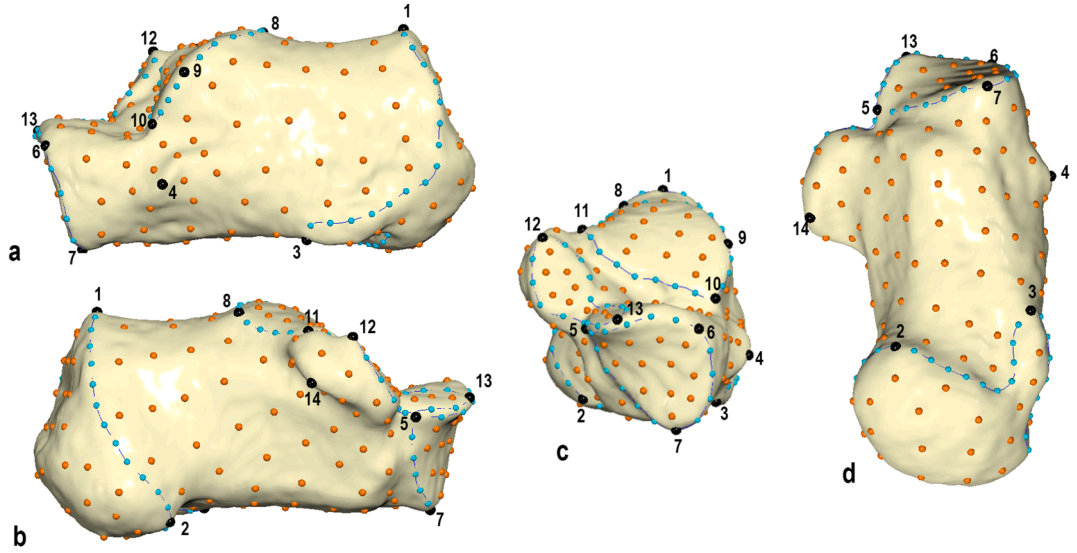

Figure 1. Template configuration of landmarks and semilandmarks on the calcaneus as seen in lateral (a), medial (b), distal (c), and plantar (d) views. These include 14 landmarks (black spheres), 85 curve semilandmarks (blue spheres), and 177 surface semilandmarks (orange spheres). Description of landmarks, curves and surfaces are provided in SOM Table S1. (For interpretation of the references to color in this figure legend, the reader is referred to the web version of this article.)

SDR-112 were acquired using a structured light scanner and provided from the Group of Paleoanthropology, Department of Paleobiology, Museo Nacional de Ciencias Naturales-CSIC (Madrid, Spain). The Spy 2 calcaneus was scanned using an Olympus E10 camera and obtained from Neanderthal Studies Professional Online Service (http://www.archiv.neanderthal.de). The μCT image data for Qafzeh and Skhul individuals, and for Dolní Věstonice 15, were acquired using a BIR ACTIS high-resolution CT scanner at the Department of Human Evolution, Max Planck Institute for Evolutionary Anthropology (Leipzig, Germany) with voxel sizes 0.029–0.054 mm. Surface scans of the Arene Candide sample were taken using the structured light scanner DAVID® SLS-2 (DAVID Group 2007–2015) and downloaded from a Morphosource database labeled 'The Arene Candide 3D Database' (https://www.morphosource.org/projects/00000C206). Calcanei of San Teodoro 1, Baucina, and the Bologna sample were scanned using an Artec Space Spider 3D structured light laser scanner (point-accuracy = 0.05 mm; mesh resolution = 0.1 mm) housed at the Department of Biological, Geological and Environmental Sciences of the University of Bologna. The Bologna sample is stored in the Morphosource database 'The Virtual DHOC of the Certosa Cemetery of Bologna' (https://www.morphosource.org/projects/000610808).

2.3. Geometric morphometrics and statistical analyses

A 3D template of 14 landmarks, 85 curve semilandmarks, and 177 surface semilandmarks (Fig. 1; Supplementary Online Material [SOM] Table S1) was created in Viewbox 4 software (dHAL software, Kifissia) on a specimen of the DHOC of the University of Bologna (Sorrentino et al., 2025). This set of landmarks and semilandmarks permitted capturing the whole morphology of the calcaneus, as well as isolating and analyzing calcaneal articular facets (i.e., joined anterior and posterior talar facets, and the cuboid facet, respectively) and the calcaneal tuberosity. The template was applied to all individuals of the sample, i.e., the targets, allowing semilandmarks to slide along curves and surfaces becoming geometrically homologous by minimizing thin-plate spline bending energy between the targets and the template (Gunz and Mitteroecker, 2013). In cases where some landmarks and/or semilandmarks lay on missing portions of a calcaneal external surface, their positions were estimated using the 'estimate.missing' function, with the thin-plate spline method, in the R package Geomorph v 4.0.1 (Adams and Otárola-Castillo, 2013). For *H. sapiens* fossil and modern individuals, this estimation was based on the overall *H. sapiens* sample, while for Neanderthal individuals, the preserved landmarks and semilandmarks were used as references for estimating the missing ones (Gunz et al., 2009). Numbers and percentages of estimated (semi)landmarks for fossil specimens are presented in SOM Table S2. Higher percentages of missing landmarks are recorded in the calcaneal tuberosity of Regourdou 1, Spy 2, La Chapelle, SD 2192, and SDR 112, as well as in the cuboid facet of Regourdou 1 and Spy 2. In contrast, the anterior and medial talar facets, as well as the posterior talar facet, are relatively well preserved and show fewer estimated missing data (SOM Table S2).

Although sexual dimorphism may affect calcaneal shape (Moore et al., 2019; Nozaki et al., 2020; Dann et al., 2024), the distribution of sexes within the groups does not allow for a statistical assessment of sex-related differences within groups. Therefore, individuals of all sexes were pooled within each taxon/group for the analyses. Four separate generalized Procrustes analyses were performed on the Cartesian coordinates of the respective whole calcaneus, the talar facets, the cuboid facet, and the tuberosity using the R package Geomorph v 4.0.1 with semilandmarks being allowed to slide with each recursive update of the Procrustes consensus (Slice, 2006).

For each set of Procrustes coordinates, a series of analyses was performed. Procrustes analysis of variance (ANOVA) (in R package Geomorph v 4.0.1) was conducted using a residual randomization procedure (n = 1000), followed by a pairwise comparison, to assess the role of shape (i.e., Procrustes coordinates), size (natural logarithm of centroid size), and allometry (shape:size) in determining groups' differences. Shape variation was explored and visualized through principal component analysis (PCA). Differences among groups along the principal components (PCs) contributing to >5% of variance were assessed using one-way ANOVA accompanied with the Tukey post hoc or Kruskal-Wallis test with Mann-Whitney U intergroup comparisons when data did not pass a normality test (i.e., assessed using a Shapiro test). Differences in the natural logarithm of centroid size, used as a proxy for respective size of the whole calcaneus, the talar facets, the cuboid facet, and the tuberosity, were assessed using one-way ANOVA or Kruskal-Wallis tests (based on a normal distribution of the sample) and visualized with boxplots (Sorrentino et al., 2023).

All statistical tests were performed in R v. 4.4.2.

Table 2
Procrustes analyses of variance (ANOVAs[a]) for the whole calcaneus, tuberosity, talar facets, and cuboid facet.

Variables	Df	SS	MS	R^2	F	Z	p value
Whole calcaneus							
Species	4	0.12126	0.030316	0.20513	4.3316	5.7553	**0.001**
Size	1	0.01124	0.011237	0.01901	1.6056	1.5736	0.061
Species:size	4	0.03174	0.007934	0.05369	1.1337	0.8467	0.196
Tuberosity							
Species	4	0.22907	0.057267	0.25684	5.8094	5.4543	**0.001**
Size	1	0.02322	0.023216	0.02603	2.3551	2.2537	**0.016**
Species:size	4	0.03827	0.009568	0.04291	0.9706	−0.0386	0.514
Talar facets							
Species	4	0.11022	0.027555	0.15455	2.9797	5.4581	**0.001**
Size	1	0.00682	0.006817	0.00956	0.7371	−0.6770	0.756
Species:size	4	0.03204	0.008009	0.04492	0.8661	−0.6400	0.744
Cuboid							
Species	4	0.12225	0.030563	0.10812	2.0067	3.13279	**0.001**
Size	1	0.01143	0.011433	0.01011	0.7506	−0.48271	0.672
Species:size	4	0.06799	0.016997	0.06013	1.1160	0.63653	0.259

Abbreviations: Df = degree of freedom; SS = Procrustes distance sum of squares; MS = mean squares distance; R^2 = coefficient of determination; F = effect type; Z = effect size.
[a] Significant p values (<0.05) for model terms are presented in bold.

3. Results

The Procrustes ANOVAs (number of permutations = 1000) for the whole calcaneus, as well as for the individual calcaneal facets and the tuberosity, reveal significant differences in calcaneal shape based on group or species membership (Tables 2 and 3). Tuberosity shape accounts for the greatest amount of variation in group or species membership (R^2 = 25.7%), followed by whole calcaneal shape (R^2 = 20.5%), the joined talar facets (R^2 = 15.4%), and finally the cuboid facet (R^2 = 10.8%; Table 2). No significant effects of size-driven shape variation (i.e., allometry) were detected, except for size (as indicated by the natural log of centroid size) accounting for weak differences (R^2 = 2.6%) among individuals when considering only the tuberosity (Table 2). Overall, size does not account for significant differences among the groups, considering the whole calcaneus, the individual calcaneal facets, or the tuberosity, with Neanderthals falling among *H. sapiens* ranges of size variation (SOM Fig. S1 and SOM Table S3).

Table 3
Pairwise comparisons of Procrustes ANOVA results.[a]

Region	NEA vs. BAU	NEA vs. BO	NEA vs. LUP	NEA vs. EUP	BAU vs. BO	BAU vs. LUP	BAU vs. EUP	BO vs. LUP	BO vs. EUP
Whole calcaneus	**0.001**	**0.001**	**0.001**	**0.002**	**0.040**	0.238	0.256	**0.025**	**0.036**
Tuberosity	**0.001**	**0.001**	**0.001**	**0.001**	0.095	0.461	0.098	0.819	**0.048**
Talar facets	**0.001**	**0.001**	**0.001**	0.273	**0.019**	0.137	0.071	0.072	**0.007**
Cuboid	0.124	**0.003**	**0.001**	0.089	0.090	**0.006**	0.062	**0.045**	0.476

Abbreviations: NEA = Neanderthals; EUP = early Upper Pleistocene; LUP = late Upper Pleistocene; BAU = Baucina; BO = Bologna; ANOVA = analysis of variance.
[a] Significant p values (<0.05) for model terms are presented in bold.

3.1. Whole calcaneus

The PCA plot and pairwise comparisons following the Procrustes ANOVA for the whole calcaneus show that Neanderthals are significantly different from all *H. sapiens* groups (Fig. 2, Table 3, and SOM Table S4). Neanderthal calcaneal shape diverges from those of all *H. sapiens* groups ($p < 0.001$) along the first 4 PCs (all contributing to >5% of variance; Fig. 2, SOM Fig. S2 and SOM Table S4), accounting mainly for Neanderthals having a longitudinally shorter and mediolaterally wider calcaneus, as well as a dorsoplantarly taller calcaneal corpus as clearly seen by the extreme shape accounting for negative scores of PC1 (21.1% of variance). Neanderthals also exhibit enlarged calcaneal facets and a larger tuberosity with respect to the overall calcaneal configuration (extreme shape along negative score of PC1, Fig. 2 and SOM Fig. S2), although their overall size (as indicated by the natural log of centroid size) falls within the range of variation of *H. sapiens* groups (SOM Fig. S1 and SOM Table S3). Particularly, Neanderthals combine traits such as a very short *sinus tarsi*, a laterally flatter and expanded posterior talar facet, enlarged and flatter medial and anterior talar facets, a more broad and plantarly oriented sustentaculum tali, an anteriorly positioned medial aspect of the cuboid facet relative to the rest of the calcaneus, a less projecting peroneal trochlea, and a markedly reduced lateral plantar process of the tuberosity (Fig. 2 and SOM Fig. S3).

Despite overlap among the *H. sapiens* groups in the PCA plot (Fig. 2), calcanei of the postindustrial group from Bologna are significantly different from those of all other *H. sapiens* groups (EUP, LUP, and the Iron Age population; Table 3 and SOM Table S4). Shape differences between Bologna calcanei and those of early and late hunter-gatherer *H. sapiens* groups are mainly detected along PC4 (6.6% of variance; SOM Fig. S2), while the Iron Age group does not differ from any other group along PC4 (SOM Table S4). Bologna modern humans differ from EUP and LUP *H. sapiens* by showing a mediolaterally broader calcaneal tuberosity in plantar view, a less mediolaterally expanded posterior talar facet, and a less elongated medial talar facet and sustentaculum tali (SOM Figs. S2 and S3).

3.2. Tuberosity

Neanderthals clearly differ from all *H. sapiens* groups (Table 3), and this difference is mainly captured by PC1 (33.3% of variance; Fig. 3 and SOM Table S5). Negative scores on PC1 (i.e., Neanderthals) correspond to an oval shape of the tuberosity in proximal view with a mediolaterally enlarged superior aspect of the tuberosity and a very short lateral plantar process that is also slightly projected

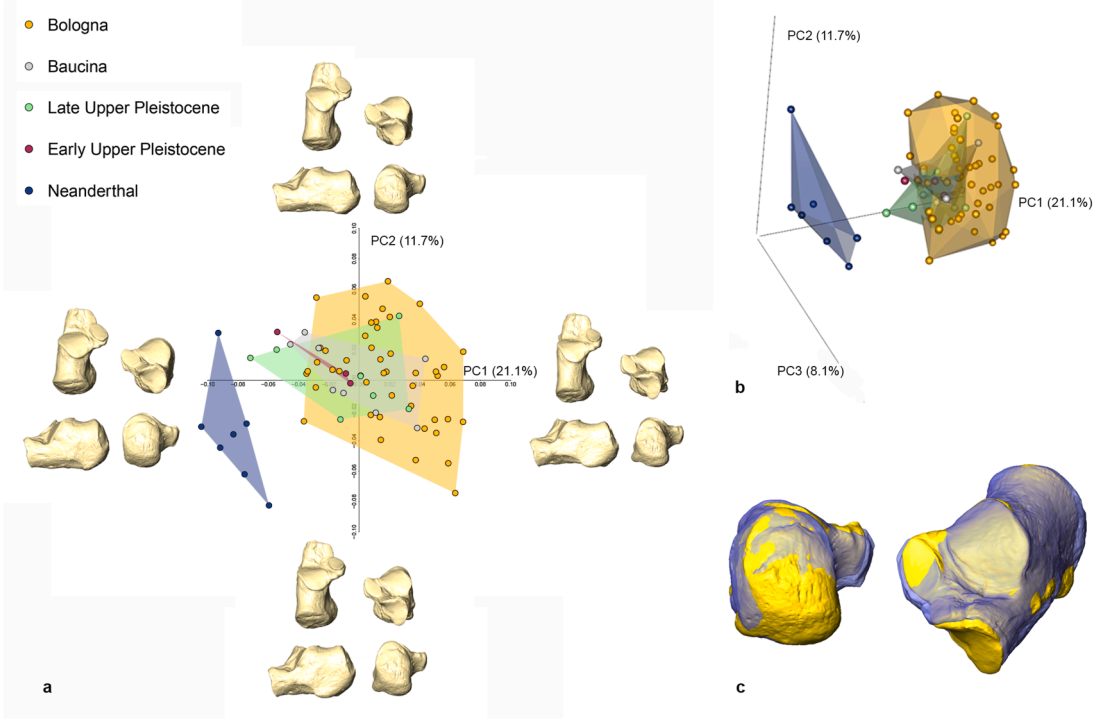

Figure 2. Principal component analysis (PCA) plots of the whole calcaneus showing PC1 vs. PC2 (a) and the first 3 PCs (b). Shape changes along the PC axes are illustrated in dorsal (top left), distal (top right), lateral (bottom left), and proximal (bottom right) views. Morphological differences between the Neanderthal mean (blue transparent) and *Homo sapiens* mean (yellow) are shown in proximal (left) and distolateral (right) views (c). PC = principal component. (For interpretation of the references to color in this figure legend, the reader is referred to the web version of this article.)

toward the plantar side. Calcanei from all *H. sapiens* groups, on the other hand, exhibit a more triangular shape in proximal view. The *H. sapiens* groups also exhibit a high degree of variation in the superior aspect of tuberosity shape, ranging from an enlarged to a more narrow shape. However, in all cases, the *H. sapiens* individuals have an anteriorly extended and plantarly projecting lateral plantar process (Fig. 3, Table 3 and SOM Table S5).

3.3. Talar facets

Morphology and spatial arrangement (e.g., relative positions) of the posterior talar facet and the joined anterior and medial talar facets reveal that Neanderthals significantly differ from all *H. sapiens* groups except EUP *H. sapiens* (Table 3). Neanderthals share with EUP *H. sapiens* a relatively short *sinus tarsi* (with Neanderthals having the shortest one), a more medially convex posterior talar facet, and an enlarged medial talar facet that is more posteriorly oriented (Fig. 4 and SOM Fig. S3). Still, Neanderthal calcanei show some distinctive traits, such as a laterally flatter and expanded posterior talar facet and enlarged medial and anterior talar facets. Shape differences among *H. sapiens* groups are only slightly captured by PC1 (14.9% of variance), which mainly highlights differences between EUP *H. sapiens* and the Baucina and Bologna groups (Fig. 4 and SOM Table S6). However, a trend is detectable from highly mobile EUP *H. sapiens* to the postindustrial group from Bologna, with the most recent and sedentary group showing a more anteroposteriorly extended posterior talar facet, and a medial talar facet that is reduced in surface area and more anteriorly oriented (Fig. 4 and SOM Fig. S3).

3.4. Cuboid facet

The cuboid facet accounts for the smallest amount of variation among species/groups (see R^2 in Table 2). Neanderthals differ from Bologna and LUP *H. sapiens*, and LUP *H. sapiens* differ from both Bologna and Baucina groups (Table 3). No statistical differences were detected along the first five PCs, all of which contribute more than 5% of the total variance (SOM Table S7). However, the PCA plot (Fig. 5) shows a tendency for separation of Neanderthals from both EUP and LUP *H. sapiens* groups along PC2, as well as between the EUP and LUP *H. sapiens* groups themselves. The Bologna group exhibits substantial variance, causing it to overlap with all other groups. Negative scores of PC2, such as those exhibited by Neanderthal calcanei, appear to be characterized by a relatively flatter and shorter cuboid facet (Fig. 5 and SOM Fig. S3). The cuboid facet becomes progressively more superoinferiorly concave and taller toward positive scores of PC2, reaching its highest concavity and height in Bologna calcanei (Fig. 5 and SOM Fig. S3).

4. Discussion

Previous studies have identified similarities between Neanderthals' foot bones and those of *H. sapiens* (Trinkaus, 1975, 1983). More recent studies have observed marked differences between Neanderthal and *H. sapiens* foot bones that are not only related to increased robusticity associated with more substantial biomechanical demands and greater body mass of the former but that are also thought to reflect anatomical functional adaptations linked to different foot postures and potentially also phylogenetic heritage (Pablos et al., 2017; Rosas et al., 2017; Pearson et al., 2020; Sorrentino et al., 2021, 2023; Pablos and Arsuaga, 2024). The present study uses a geometric morphometric approach to identify which calcaneal traits of Neanderthals and *H. sapiens* may be plesiomorphic, autapomorphic, and/or functional by analyzing whole calcaneal shape as well as individual shapes of calcaneal articular facets and the tuberosity.

4.1. Robusticity and functional adaptations

Whole calcaneal shape of Neanderthals differs from that of *H. sapiens* (both early and recent) by having a longitudinally

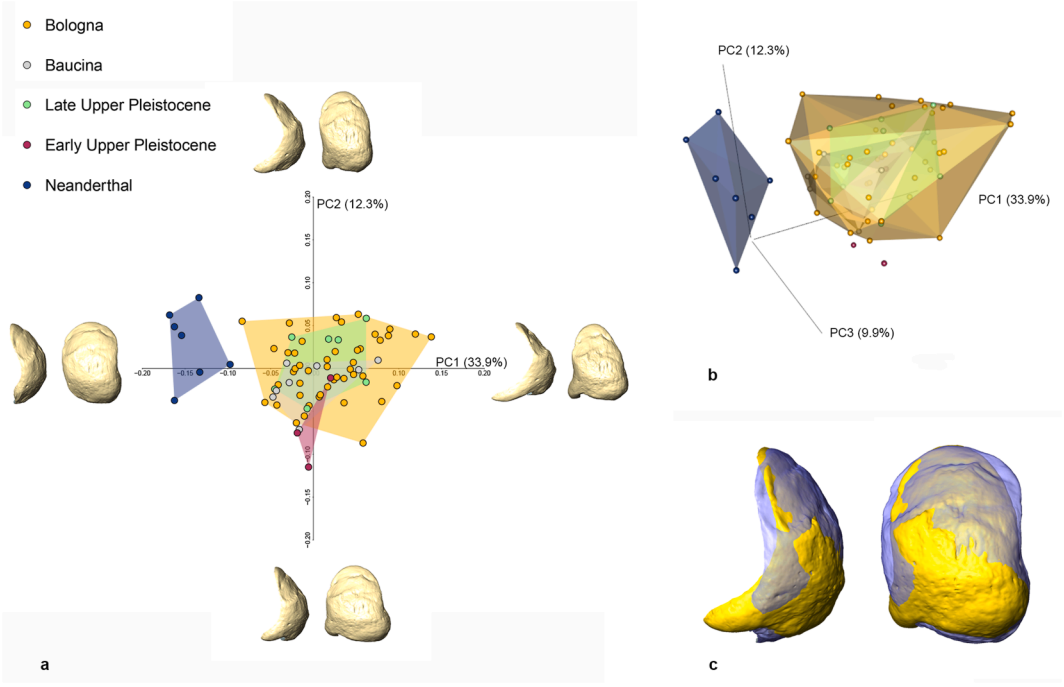

Figure 3. Principal component analysis (PCA) plots of the tuberosity showing PC1 vs. PC2 (a) and the first 3 PCs (b). Shape changes along the PC axes are illustrated in lateral (left) and proximal (right) views. Morphological differences between the Neanderthal mean (blue transparent) and *Homo sapiens* mean (yellow) are shown in lateral (left) and proximal (right) views (c). PC = principal component. (For interpretation of the references to color in this figure legend, the reader is referred to the web version of this article.)

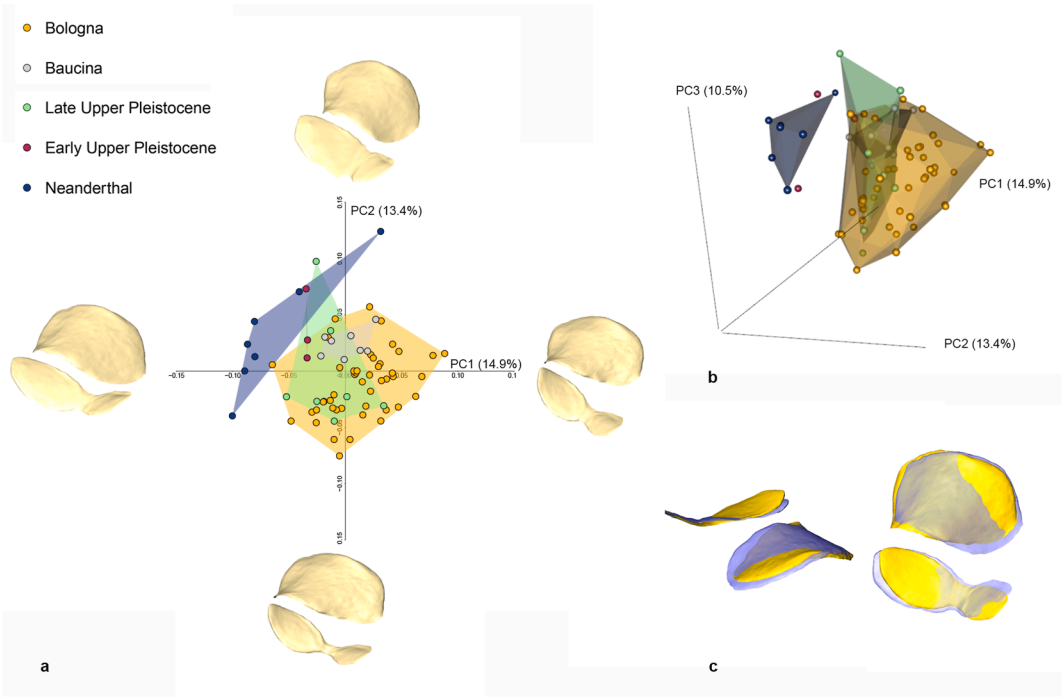

Figure 4. Principal component analysis (PCA) plots of the talar facets showing PC1 vs. PC2 (a) and the first 3 PCs (b). Shape changes along the PC axes are illustrated in proximodorsal view. Morphological differences between the Neanderthal mean (blue transparent) and *Homo sapiens* mean (yellow) are shown in proximolateral (left) and dorsal (right) views (c). PC = principal component. (For interpretation of the references to color in this figure legend, the reader is referred to the web version of this article.)

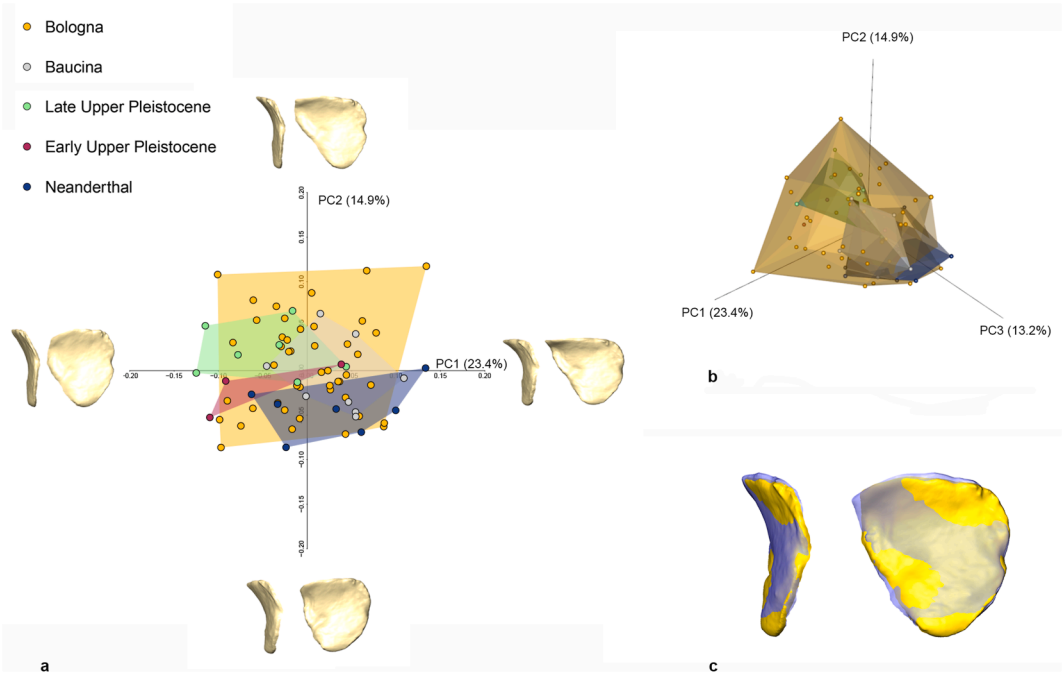

Figure 5. Principal component analysis (PCA) plots of the cuboid facet showing PC1 vs. PC2 (a) and the first 3 PCs (b). Shape changes along the PC axes are illustrated in lateral (left) and distal (right) views. Morphological differences between the Neanderthal mean (blue transparent) and *Homo sapiens* mean (yellow) are shown in lateral (left) and distal (right) views (c). PC = principal component. (For interpretation of the references to color in this figure legend, the reader is referred to the web version of this article.)

shorter and mediolaterally wider calcaneus and a dorsoplantarly taller calcaneal body. It has been shown that in apes, the overall calcaneus scales with body size, while some traits still vary based on locomotor behaviors (Prang, 2015a, 2015b, 2024; Harper et al., 2021, 2022a; Harper, 2023). A recent study on shape-size relationships in the modern human calcaneus suggested that as the calcaneus increases in size, it becomes taller, wider, and relatively shorter, likely enabling more effective mitigation of stresses from gravitational and muscular forces that also scale with size (Treherne et al., 2025). Broad calcanei in both Neanderthals and

Sima de los Huesos hominins have been suggested to represent robusticity linked to their greater body mass. However, metrical variables show a different pattern for calcaneal length, which does not differ significantly between Neanderthals and either fossil or recent *H. sapiens* but becomes significantly different when body length is considered instead (Trinkaus, 1983; Pablos et al., 2014, 2017; Pablos and Arsuaga, 2024).

Notably, the widening and increased height of the Neanderthal calcaneal body (i.e., shape related characteristics) may also reflect adaptations to an active lifestyle and unshod locomotion, similar to those features observed in *H. sapiens* hunter-gatherers (Harper, 2023). A similar pattern has been observed for metrical variables. Specifically, the medial width (or the width of the sustentaculum tali) and calcaneal height of Neanderthals and Sima de los Huesos hominins do not differ significantly from those of fossil *H. sapiens*, although they differ significantly from modern human comparative samples (Pablos et al., 2014, 2017; Pablos and Arsuaga, 2024). Nonetheless, a certain degree of variability in these relationships can be present within *H. sapiens* based on the population being studied (Dann et al., 2024). In the present study, we observed that aspects of calcanei of highly mobile *H. sapiens* groups (EUP and LUP hunter-gatherers and the mixed farmers/foragers of Baucina) tended to resemble those of Neanderthals more closely than the more sedentary postindustrial group from Bologna. A relatively narrower calcaneal body, on the other hand, is more pronounced in LUP hunter-gatherers than in the Bologna group, confirming important variability within our species (Fig. 2, SOM Figs. S2 and S3, SOM Table S4). A mediolaterally narrowed and dorsoplantarly shortened calcaneal body in *H. sapiens* also could signal gracilization resulting from a more sedentary lifestyle and cultural innovation (i.e., use of shoes), reflecting the overall skeletal gracilization observed in the group (Carlson and Marchi, 2014; Chirchir et al., 2015; Ryan and Shaw, 2015). However, additional factors such as ancestry, nutrition, and environment also have been shown to contribute to calcaneal shape variation in *H. sapiens* (Dann et al., 2024).

Calcaneal length tends to increase with decreasing levels of inferred mobility in the *H. sapiens* groups (Fig. 2, SOM Figs. S2 and S3). A comparative biomechanical study on foot mechanics and proportions have associated a shorter rearfoot length with improved muscle efficiency and enhanced performance in acceleration during sprinting (Baxter et al., 2012). The relatively shorter calcaneus observed in *H. sapiens* hunter-gatherers would favor a shorter calcaneal tuber, likely offering the adaptive benefits these features provide during running and fast walking (Raichlen et al., 2011; Harper, 2023). Some functional adaptations in modern humans are also relatively recent developments, as shown by significant increases in calcaneal length in postmedieval populations compared to medieval ones, with variation according to sex (Albee, 2022).

Although a shortened rearfoot might suggest that Neanderthals had enhanced running capabilities, Raichlen et al. (Raichlen et al., 2011) emphasized the importance of the length of the calcaneal tuber relative to total calcaneal length. In particular, they associated longer relative length of the calcaneal tuber in Neanderthals with decreased endurance running performance. Indeed, they found that Neanderthals exhibited a proximodistally longer relative length of the calcaneal tuber (i.e., maximum distance between the edge of the calcaneal tuberosity and the anterior edge of the posterior talocalcaneal surface) than modern humans. This feature correlates with a longer Achilles tendon moment arm, where long moment arms increase not only possible joint torque but also energy costs of running at a given speed. According to Raichlen et al. (Raichlen et al., 2011), a relatively longer calcaneal tuber in Neanderthals would reflect an adaptation that increases the leverage of the plantar flexor muscles. This enhancement likely improved their torque generation capabilities when walking on uneven terrain rather than supporting economical running (Raichlen et al., 2011). This does not imply that Neanderthals were incapable of endurance running, but it suggests that endurance running had less adaptive importance in their subsistence strategy.

Therefore, the more robust calcaneus in Neanderthals—characterized by being longitudinally shorter, wider, and taller but with a relatively longer calcaneal tuber—may be necessary to accommodate their presumably increased mechanical loading associated with greater body mass and high mobility (endurance walking) on presumably uneven terrain.

4.2. Plesiomorphic traits

In addition to the functional aspects related to calcaneal length discussed earlier, it is noteworthy that a shorter calcaneal corpus characterizes the Sima de los Huesos hominins than in the case of Neanderthals (Pablos et al., 2014, 2017; Pablos and Arsuaga, 2024). This suggests a combination of inherited traits and functional adaptations distinguish Neanderthals and *H. sapiens*.

The *sinus tarsi* is also notably shorter in Neanderthals (Fig. 2 and SOM Fig. S1), reflecting their characteristically short talar neck (Rosas et al., 2017; Sorrentino et al., 2021). This anatomical feature likely reflects an ancestral (plesiomorphic) characteristic, as it is also observed in other *Homo* fossils from the Pleistocene, and it is not correlated with body mass (Lu et al., 2011; Pablos et al., 2017; Rosas et al., 2017; Sorrentino et al., 2021).

4.3. Functional traits

Morphology of the articular facets of the calcaneus provides important insights into locomotor behavior and foot function among different human populations. Since general morphology of the talar facet in Neanderthals and *H. sapiens* hunter-gatherer groups is similar, this may indicate characteristic morphology of a population that engages in high levels of physical activity (Pearson et al., 2006).

The use of footwear and levels of mobility have been linked to variation in *H. sapiens* subtalar joint shape, which is the joint primarily responsible for foot eversion and inversion (Sorrentino et al., 2020b; Harper, 2023; Dann et al., 2024). Specifically, variations in both external morphology and trabecular structure have suggested higher lateral loading on the talus in hunter-gatherer populations, likely due to a greater range of inversion and eversion and a more everted foot posture (Sorrentino et al., 2020b, 2021, 2022). This is reflected in the morphology (i.e., shape independent of size) of the talar facet of the calcaneus, where more mobile, and likely unshod, *H. sapiens* groups (especially EUP and, to a lesser extent, LUP humans) and Neanderthals present a broader and more mediolaterally expanded posterior talar facet, along with an elongated medial talar facet and sustentaculum tali, all of which facilitate inversion-eversion motions (Figs. 2 and 4, and SOM Figs. S2 and S3). A mediolaterally expanded posterior talar facet morphology allows for greater contact surface with the posterior calcaneal facet of the talus, thereby providing a larger surface area to distribute loads through the subtalar joint, ultimately reducing the maximum or peak stresses and enhancing ability to withstand higher forces in a close-packed joint position during locomotion (Harper, 2023). Moreover, this subtalar joint configuration may reflect an adaptation to a larger inversion-eversion range of motion during walking on uneven surfaces (Apolito et al., 2025). In contrast, the Bologna postindustrial group exhibits a less mediolaterally expanded posterior talar facet, a less

elongated medial talar facet, and a less-prominent sustentaculum tali, collectively suggesting the Bologna group exhibits a different loading distribution and a more limited range of inversion-eversion motion, as seen in habitually shod populations (Zipfel and Berger, 2007; Holowka et al., 2022). In particular, a more anteroposteriorly extended posterior talar facet in the Bologna group (Fig. 4 and SOM Fig. S3) may indicate an increased emphasis on plantarflexion and dorsiflexion capabilities, which would be consistent with the use of rigid footwear that tends to constrain rearfoot eversion (Trudeau et al., 2017).

Shape of the isolated cuboid facet accounts for the smallest differences among species and groups (Tables 2 and 3). The Neanderthal cuboid facet is flatter and shorter than that of *H. sapiens*. In the latter groups, the cuboid facet becomes taller and more superoinferiorly concave from the most mobile hunter-gatherers to the most sedentary groups (Fig. 5 and SOM Fig. S3). Among postindustrial *H. sapiens* populations, the taller and more superoinferiorly concave cuboid facet likely reflects the influence of footwear that restricts mediolateral foot motion, limiting transverse plane movements (Harper, 2023).

4.4. Autapomorphic traits

Besides the functional implications of the shape of the talar facets of the calcaneus, it is worth noting that metrical variables also indicate that the posterior talar articular surface is broader in Neanderthals and EUP samples than in recent *H. sapiens* samples (Pablos et al., 2019). However, in the Sima de los Huesos sample (Pablos et al., 2014), this dimension is smaller and more similar to that of recent *H. sapiens*. This suggests the presence of autapomorphic characteristics in addition to those related to physical activity. Indeed, calcaneal configuration and morphology of the talar facets in Neanderthals reflect, as expected, subtalar autapomorphic traits highlighted in the talus (Sorrentino et al., 2021). The Neanderthal posterior talar facet of the calcaneus is more laterally flattened and expanded, while the medial and anterior talar facets of Neanderthal calcanei are entirely enlarged and flattened with respect to the calcanei of all *H. sapiens* groups (Figs. 2 and 4, and SOM Fig. S3). This configuration reflects the Neanderthal talus, which is characterized by higher load-bearing on its lateral side, as suggested by widened surface area and lateral distribution of high trabecular bone density throughout the posterior calcaneal facet (Pablos et al., 2017; Sorrentino et al., 2021). Correspondence between the calcaneus and talus would be expected for support of the hypothesis that Neanderthals may have had a habitually pronated foot posture (Sorrentino et al., 2021). Indeed, in modern humans, pronation allows for wider contact areas at the posterior (talar and calcaneal) facets than what is observed in supination, thus suggesting an enhanced capability to withstand load in the joint with a pronated foot (Wagner et al., 1992). A recent study on modern foot kinematics confirms that the calcaneus (relative to the talus) moves mainly during foot pronation, resulting in calcaneal eversion that is amplified under the effect of increasing load (Conconi et al., 2024). Collectively, these findings support the interpretation that the pronated foot is functionally better adapted to sustain higher loads, a condition that may also characterize Neanderthals, who are associated with greater body mass than *H. sapiens*.

Compared to *H. sapiens* groups, the Neanderthal cuboid facet is positioned differently relative to the rest of the calcaneus, with its medial side oriented more anteriorly than the rest of the calcaneus (Fig. 2 and SOM Fig. S3). This characteristic where the cuboid facet would accommodate the cuboid plantomedially, ensuring close-packed position of the calcaneocuboid joint during pronation, has not been observed in calcanei of the Jinniushan hominin or those from Sima de Los Huesos (Lu et al., 2011; Pablos et al., 2014, 2017; Pablos and Arsuaga, 2024). This unique configuration in Neanderthals may represent a plastic response to their foot posture rather than representing an ancestral trait. For example, a more anteriorly positioned medial side of the cuboid facet has been recognized in nonhuman apes and is thought to reflect their greater midtarsal mobility at toe-off (Harper et al., 2021). This ability likely promotes a more everted cuboid facet in nonhuman apes, which can accentuate stable contact of the forefoot and toes with a substrate during terrestrial locomotion despite an inverted hind foot (Nozaki et al., 2021).

During inversion, a closed-packed position of the calcaneocuboid joint is thought to contribute to transforming the *H. sapiens* foot into a rigid lever during toe-off and serve to stabilize the lateral longitudinal arch of the foot (Desilva et al., 2015; Harper et al., 2021). The position of the cuboid facet in Neanderthals may suggest comparatively less stability during this portion of stance phase of the gait cycle. However, a less concave surface would contribute to reducing range of motion at the calcaneocuboid joint, perhaps acting as a compensatory mechanism for achieving a similar closed-packed position in Neanderthals, therefore serving to enhance stability using a different mechanism. If a fully rigid lever was not achieved, this would be suggestive of a potentially different expression of the lateral longitudinal arch in Neanderthals. Clinical studies have reported associations between flatfoot conditions and the calcaneocuboid joint, although there is limited direct evidence linking the shape of the cuboid facet itself (for example, if the surface is more concave or flattened) to flatfoot conditions (Fallon Verbruggen et al., 2023). Kinematic studies have suggested that, in weight-bearing, modern humans experience calcaneocuboid abduction, and when it increases, it causes a flattening of the lateral longitudinal arch (Conconi et al., 2024). Thus, Neanderthals may have experienced a lower lateral longitudinal arch than *H. sapiens* and a certain degree of mobility in the midfoot region, which would likely help maintain stability while navigating uneven terrain.

This hypothesis on the Neanderthal lateral longitudinal arch echoes recent findings on the morphology of the navicular bone, considered the keystone of the medial longitudinal arch, where Neanderthals share some features (e.g., projecting tuberosity, a more concave talar facet, and a greater anterior convexity of the navicular) with adults clinically diagnosed with acquired flexible flatfoot, most of whom were clinically overweight or obese (Sorrentino et al., 2023). In recent humans, it appears that greater body mass may be the cause of pronated foot postures, ultimately leading to flattening of the longitudinal arches in these individuals (Butterworth et al., 2015). A similar explanation may exist in Neanderthals, where their body mass could have played a crucial role in foot stability and longitudinal arch expression. In addition to body mass, another potential contributing factor to this foot posture in Neanderthals could be favoring stereotyped loadings in natural terrains. Ultimately, both stiffness and mobility of the midfoot contribute to foot function, e.g., a greater range of eversion-inversion helps in maintaining balance during uneven surface walking (Holowka et al., 2017; Apolito et al., 2025).

Different strategies for enhancing foot stabilization and force transmission through proximal tarsal joints are also observed in the shape of the Neanderthal calcaneal tuberosity. The oval shape of the tuberosity in Neanderthals appears derived. This shape is formed by a mediolaterally enlarged superior aspect of the tuberosity and a very short lateral plantar process that is also slightly projected toward the plantar side (Figs. 2 and 3, and SOM Fig. S3). The oval shape of the Neanderthal tuberosity, in contrast with the more triangular shape seen in *H. sapiens*, is the result of

reduced tuberosity height and decreased widening of the base compared to the rest of the calcaneus in the former. This configuration likely resembles those seen in asymptomatic planus feet vs. cavus feet (Moore et al., 2019). An enlarged superior aspect of the tuberosity may be related to the attachment area and actions of the triceps surae and Achilles tendon. Modern humans with flatfoot can be associated with a short or contracted Achilles tendon (Mosca, 2010), which would likely influence the morphology of the tuberosity, although this has not been tested.

The lateral plantar process of the Neanderthal calcaneal tuberosity is poorly developed and plantarly projecting. Medial and lateral plantar processes are usually positioned in the same transverse plane in *H. sapiens*, being more plantarly positioned than in other apes, although there is size and positional variation within modern humans (Boyle et al., 2018). Both processes serve as attachment sites for the long plantar ligament and intrinsic foot muscles (i.e., quadratus plantae and flexor digitorum brevis), both of which are crucial for foot movement and stability of the plantar arch (Mckeon et al., 2015). Additionally, the lateral plantar process is a weight-bearing structure in *H. sapiens* that plays a key role in dissipating stresses generated by ground reaction forces during heel strike (Latimer et al., 1987; Latimer and Lovejoy, 1989; Koneru and Harper, 2024). A less developed lateral plantar process in Neanderthals may suggest that the long plantar ligament was less effective at maintaining the longitudinal arch than the condition in modern humans, potentially indicating increased foot mobility as an adaptation to uneven terrain in the former. A similar hypothesis has been suggested for the Jinniushan calcanei that are characterized by a different shape of the lateral plantar process (i.e., laterally disposed and anteriorly shifted) with respect to modern humans (Lu et al., 2011). Compared to Jinniushan (Lu et al., 2011), Neanderthals exhibit maximal reduction of the lateral plantar process, indicating it may be an adaptation to their unique foot posture and weight-bearing demands. However, because this feature was not reported in descriptions of the Sima de los Huesos sample (Pablos et al., 2014, 2017; Pablos and Arsuaga, 2024), no firm conclusions can be drawn regarding the morphological diversity of the lateral plantar process among Middle Pleistocene hominins. Consequently, further assessment is required to determine whether this trait should be interpreted as autapomorphic.

Additionally, a less developed peroneal trochlea in Neanderthals (Fig. 2) would suggest a decreased role of the peroneal musculature in an everted foot posture (Stern and Susman, 1983; Gill et al., 2014). Indeed, development of the lateral plantar process and that of the peroneal trochlea have been positively correlated, and it has been suggested that modern humans with large peroneal trochleae also have high longitudinal arches and vice versa (Gill et al., 2014). Nonhuman apes have relatively larger peroneal trochleae than modern humans despite having flat feet, suggesting that the functional significance of an enlarged peroneal trochlea differs between species, which complicates its interpretation in human ancestors (Gill et al., 2014; Prang, 2015a, 2015b; McNutt et al., 2017; Boyle et al., 2018; Harper et al., 2021; Nozaki et al., 2021).

Altogether, these traits offer some support for the hypothesis that Neanderthals had a pronated foot and, consequently, a different load-bearing and force dissipation regime in the foot, resulting likely from different anatomical expressions of their longitudinal arches (Sorrentino et al., 2021, 2023). While these features add another piece to the puzzle of understanding differences in Neanderthal foot bones from those of *H. sapiens*, the suggestive hypothesis of different longitudinal arches in Neanderthals and *H. sapiens* requires further investigation, auspiciously combining geometric morphometrics with 3D modeling kinematic analysis.

4.5. Conclusions

In conclusion, this study supports unique locomotor adaptations in Neanderthals, along with inherited traits and biomechanical demands associated with their greater body mass and activity levels. Compared to *H. sapiens*, Neanderthals exhibit a more robust calcaneus: one that is shorter in length, wider mediolaterally, and taller dorsoplantarly, likely reflecting adaptations for increased load-bearing and high mobility. Similar traits, but to a lesser extent, are also observed in highly mobile, unshod *H. sapiens* groups, whereas more gracile calcanei characterize sedentary, postindustrial populations—likely due to footwear use and reduced mobility on the landscape. Anatomical traits like a shorter *sinus tarsi* in Neanderthals may reflect ancestral characteristics. Notably, the subtalar joint in Neanderthals—characterized by flatter and more laterally expanded posterior talar facets—and a reoriented calcaneocuboid joint support the hypothesis of habitually pronated foot posture in Neanderthals. Differences in shape and orientation of the cuboid facet and the calcaneal tuberosity suggest alternative strategies for foot stabilization and load dissipation, possibly indicating a distinct expression of the longitudinal arch in Neanderthals. Based on our findings, it is plausible that the Neanderthal talar articular facets and calcaneocuboid joint, together with tuberosity shape, contributed to a unique, habitually pronated foot posture that supported greater body mass and accommodated the high biomechanical demands of Neanderthal locomotion.

The unique external calcaneal morphology observed in Neanderthals raises fundamental questions regarding its ontogenetic basis. While our study focuses on adult morphology, these pronounced interspecific divergences likely reflect distinct developmental pathways, shaped by both intrinsic (genetic, epigenetic) and extrinsic (biomechanical loading) factors throughout growth. For instance, recent work on modern human calcaneal ontogeny highlights how specific regions of this bone undergo significant shape changes also in response to bipedal gait acquisition and increasing weight-bearing demand (Figus et al., 2025). Such insights into human developmental trajectories provide a crucial interpretive framework, suggesting that the distinct Neanderthal calcaneal shape may stem from a unique developmental program or from different responses to specific locomotor demands during their growth or from a combination of both.

Altogether, these morphological patterns suggest that Neanderthals possess calcaneal anatomy that was well suited for their high-activity lifestyle and body structure. While plastic responses to activity and footwear partly explain variation in *H. sapiens*, some Neanderthal traits appear derived and may be linked to phylogenetic divergence. These findings highlight the complex interplay of functional morphology, lifestyle, and evolutionary history in shaping Neanderthal foot bones.

Declaration of competing interest

All other authors declare they have no competing interests.

Acknowledgments

We thank the curators and collections managers of the sample used in this study: F. Détroit, D. Hervé, A. Balzeau, P. Mennecier, and A. Froment (Museum National d'Histoire Naturelle, Département Hommes, Natures, Sociétés) for providing digital models of La Ferrassie 1 and 2, and La Chapelle; R. Macchiarelli, A. Mazurier, and V. Volpato (University of Poitiers) for the μCT scan of Regourdou calcaneus performed at the European Synchrotron Radiation Facility, Grenoble, France; Max Planck Institute for

Evolutionary Anthropology for access to Qafzeh 8 and 9, Skhul 4, and Dolní Věstonice 15; Museo di Paleontologia 'Gemmellaro,' Palermo (Italy), for access to San Teodoro 1; all of the people working at the El Sidrón collection for their effort and interest; Soprintendenza Archeologia, Belle Arti e Paesaggio per la città metropolitana di Genova e le province di Imperia, La Spezia e Savona provided access to Arene Candide appearing in Sparacello et al. (2018a), the collection of which was funded by Marie Curie European Union COFUND/Durham Junior Research Fellowship (under EU grant agreement number 267209), and by the Wolfson Institute for Health and Wellbeing, Durham, UK, the files were downloaded from www.MorphoSource.org, Duke University.

Access to the Spy 2 sample was made possible by the Neanderthal Studies Professional Online Service Database (https://www.nespos.org/display/openspace/Home). This work was funded by the Spanish Ministry of Science and Innovation through the projects PID2021-122356NB-I00 to A.R.

Author contributions

Rita Sorrentino: Writing – review & editing, Writing – original draft, Visualization, Software, Methodology, Investigation, Formal analysis, Data curation, Conceptualization. **Silvia Volpe:** Writing – review & editing, Visualization, Validation, Investigation, Formal analysis, Data curation. **Kristian J. Carlson:** Writing – review & editing, Validation, Supervision, Investigation, Conceptualization. **Teresa Nicolosi:** Writing – review & editing, Validation, Investigation, Data curation. **Carla Figus:** Writing – review & editing, Validation, Methodology, Data curation. **Vitale Sparacello:** Writing – review & editing, Validation, Data curation. **Francesca Meli:** Writing – review & editing, Data curation. **Michele Conconi:** Writing – review & editing, Validation, Investigation. **Nicola Sancisi:** Writing – review & editing, Validation, Investigation. **Claudio Belvedere:** Writing – review & editing, Validation, Investigation. **Alberto Leardini:** Writing – review & editing, Validation, Investigation. **Jean-Jacques Hublin:** Writing – review & editing, Resources, Data curation. **Timothy Ryan:** Writing – review & editing, Validation, Investigation. **Luca Sineo:** Writing – review & editing, Validation, Investigation, Data curation. **Antonio Rosas:** Writing – review & editing, Validation, Investigation, Funding acquisition, Data curation. **Stefano Benazzi:** Writing – review & editing, Validation, Supervision, Methodology, Investigation. **Maria Giovanna Belcastro:** Writing – review & editing, Validation, Supervision, Resources, Investigation, Data curation.

Supplementary Online Material

Supplementary Online Material related to this article can be found at https://doi.org/10.1016/j.jhevol.2026.103887.

References

Adams, D.C., Otárola-Castillo, E., 2013. Geomorph: An r package for the collection and analysis of geometric morphometric shape data. Methods Ecol. Evol. 4, 393–399.
Albee, M.E., 2022. Tarsal metric trends over the Medieval-Post-Medieval transition in London. Homo 73, 33–47.
Apolito, Z.M., Palmisano, K.G., Holowka, N.B., 2025. The adaptive function of the human ankle joint complex during walking on uneven terrains with implications for hominin locomotion. J. Hum. Evol. 203, 103678.
Baxter, J.R., Novack, T.A., Werkhoven, H. Van, Pennell, D.R., Piazza, S.J., 2012. Ankle joint mechanics and foot proportions differ between human sprinters and non-sprinters. Proc. Biol. Sci. 279, 2018–2024.
Belcastro, M.G., Bonfiglioli, B., Pedrosi, M.E., Zuppello, M., Tanganelli, V., Mariotti, V., 2017. The history and composition of the identified human skeletal collection of the Certosa Cemetery (Bologna, Italy, 19th–20th Century). Int. J. Osteoarchaeol. 27, 912–925.
Belcastro, M.G., Mariotti, V., Pietrobelli, A., Sorrentino, R., García-Tabernero, A., Estalrrich, A., Rosas, A., 2020. The study of the lower limb entheses in the Neanderthal sample from El Sidrón (Asturias, Spain): How much musculoskeletal variability did Neanderthals accumulate? J. Hum. Evol. 141, 102746.
Belvedere, O., Burgio, A., Bordonaro, G., Forgia, V., 2016. Baucina–Monte Falcone 2014, Indagini nella necropoli. Notiziario Archeologico della Soprintendenza di Palermo 18.
Bennett, M.R., Bustos, D., Pigati, J.S., Springer, K.B., Urban, T.M., Holliday, V.T., Reynolds, S.C., Budka, M., Honke, J.S., Hudson, A.M., Fenerty, B., Connelly, C., Martinez, P.J., Santucci, V.L., Odess, D., 2021. Evidence of humans in North America during the Last Glacial Maximum. Science 373, 1528–1531.
Bonifay, E., 1964. La grotte du Regourdou (Montignac, Dordogne). Stratigraphie et industrie lithique mousterienne. L'Anthropologie 68, 49–64.
Boyle, E.K., McNutt, E.J., Sasaki, T., Suwa, G., Zipfel, B., DeSilva, J.M., 2018. A quantification of calcaneal lateral plantar process position with implications for bipedal locomotion in *Australopithecus*. J. Hum. Evol. 123, 24–34.
Brzobohatá, H., Prokop, J., Horák, M., Jančárek, A., Velemínská, J., 2012. Accuracy and benefits of 3D bone surface modelling: A comparison of two methods of surface data acquisition reconstructed by laser scanning and computed tomography outputs. Coll. Antropol. 36, 801–806.
Butterworth, P.A., Urquhart, D.M., Landorf, K.B., Wluka, A.E., Cicuttini, F.M., Menz, H.B., 2015. Foot posture, range of motion and plantar pressure characteristics in obese and non-obese individuals. Gait Posture 41, 465–469.
Carlson, K.J., Grine, F.E., Pearson, O.M., 2007. Robusticity and sexual dimorphism in the postcranium of modern hunter-gatherers from Australia. Am. J. Phys. Anthropol. 134, 9–23.
Carlson, K.J., Marchi, D., 2014. Reconstructing Mobility: Environmental, Behavioral, and Morphological Determinants. Springer, New York, NY.
Castejón-Molina, P., Pablos, A., 2021. Sex estimation by third metatarsals in human fossil and recent populations. Archaeol. Anthropol. Sci. 13, 209.
Citton, P., Romano, M., Salvador, I., Avanzini, M., 2017. Reviewing the Upper Pleistocene human footprints from the "Sala dei Misteri" in the Grotta della Bàsura (Toirano, northern Italy) cave: An integrated morphometric and morpho-classificatory approach. Quatern. Sci. Rev. 169, 50–64.
Chapman, T., Semal, P., Moiseev, F., Louryan, S., Rooze, M., Jan, S.V., 2013. Application of the musculo-skeletal modelling software lhpFusionBox to a paleo-anthropological problem: The Spyrou Neandertal moves! Med. Sci. 29, 623–629.
Chirchir, H., Kivell, T.L., Ruff, C.B., Hublin, J., Carlson, K.J., Zipfel, B., 2015. Recent origin of low trabecular bone density in modern humans. Proc. Natl. Acad. Sci. 112, 366–371.
Conconi, M., Pompili, A., Sancisi, N., Durante, S., Leardini, A., Belvedere, C., 2024. Foot kinematics as a function of ground orientation and weightbearing. J. Orthop. Res. 42, 148–163.
Coutinho-Nogueira, D., Coqueugniot, H., Tillier, A.M., Nogueira, D.C., 2021. Qafzeh 9 early modern human from Southwest Asia: Age at death and sex estimation reassessed. Homo 72, 293–305.
D'Amore, G., Di Marco, S., Tartarelli, G., Bigazzi, R., Sineo, L., 2009. Late Pleistocene human evolution in Sicily: Comparative morphometric analysis of Grotta di San Teodoro craniofacial remains. J. Hum. Evol. 56, 537–550.
Dann, A., Pokhojaev, A., Anton, M., Yalovitsky, G., Kallevag-Pelleg, R., May, H., 2024. Changes in human calcaneal morphology throughout the Pleistocene-Holocene Levant. Front. Earth Sci. 12, 1294350.
De Groote, I., 2011. Femoral curvature in Neanderthals and modern humans: A 3D geometric morphometric analysis. J. Hum. Evol. 60, 540–548.
DeMars, L.J.D., Stephens, N.B., Saers, J.P.P., Gordon, A., Stock, J.T., Ryan, T.M., 2020. Using point clouds to investigate the relationship between trabecular bone phenotype and behavior: An example utilizing the human calcaneus. Am. J. Hum. Biol. 33, e23468.
DeSilva, J., McNutt, E., Benoit, J., Zipfel, B., 2019. One small step: A review of Plio-Pleistocene hominin foot evolution. Am. J. Phys. Anthropol. 168, 63–140.
DeSilva, J.M., Devlin, M.J., 2012. A comparative study of the trabecular bony architecture of the talus in humans, non-human primates, and Australopithecus. J. Hum. Evol. 63, 536–551.
DeSilva, J.M., Swanson, Z., Gill, C.M., Sobel, M., Uy, J., Gill, S.V., Bonne-Annee, R., Swanson, Z., Gill, C.M., Sobel, M., Uy, J., Gill, S.V., 2015. Midtarsal break variation in modern humans: Functional causes, skeletal correlates, and paleontological implications. Am. J. Phys. Anthropol. 156, 543–552.
Duveau, J., Berillon, G., Verna, C., Laisné, G., Cliquet, D., 2019. The composition of a Neandertal social group revealed by the hominin footprints at Le Rozel (Normandy, France). Proc. Natl. Acad. Sci. U. S. A. 116, 19409–19414.
Fallon Verbruggen, F., Killen, B.A., Burssens, A., Boey, H., Vander Sloten, J., Jonkers, I., 2023. Unique shape variations of hind and midfoot bones in flatfoot subjects—A statistical shape modeling approach. Clin. Anat. 36, 848–857.
Fernández, P.J., Mongle, C.S., Leakey, L., Proctor, D.J., Orr, C.M., Patel, B.A., Almécija, S., Tocheri, M.W., Jungers, W.L., 2018. Evolution and function of the hominin forefoot. Proc. Natl. Acad. Sci. 15, 8746–8751.
Fewlass, H., Talamo, S., Kromer, B., Bard, E., Tuna, T., Fagault, Y., Sponheimer, M., Ryder, C., Hublin, J.J., Perri, A., Sázelová, S., Svoboda, J., 2019. Direct radiocarbon dates of mid Upper Palaeolithic human remains from Dolní Věstonice II and Pavlov I, Czech Republic. J. Archaeolog. Sci. Rep. 27, 102000.
Figus, C., Carlson, K.J., Bortolini, E., Saers, J., Seghi, F., Sorrentino, R., Bernardini, F., Vazzana, A., Erjavec, I., Novak, M., Tuniz, C., Belcastro, M.G., Stock, J., Ryan, T.M., Benazzi, S., 2025. The ontogeny of the human calcaneus: Insights from morphological and trabecular changes during postnatal growth. Am. J. Biol. Anthropol. 186, e70007.

Finestone, E.M., Brown, M.H., Ross, S.R., Pontzer, H., 2018. Great ape walking kinematics: Implications for hominoid evolution. Am. J. Phys. Anthropol. 166, 43–55.
Forgia, V., Speciale, C., Ölz, M.E., Romano, A., Savarino, F., Natoli, R., Sineo, L., 2025. The human entry in Sicily: New archaeological and paleoenvironmental evidence from San Teodoro cave (Acquedolci, Messina). Archaeol. Anthropol. Sci. 17, 109.
Formicola, V., Pontrandolfi, A., Svoboda, J., 2001. The Upper Paleolithic triple burial of Dolní Věstonice: Pathology and funerary behavior. Am. J. Phys. Anthropol. 115, 372–379.
Gebo, D.L., 1992. Plantigrady and foot adaptation in African apes: Implications for hominid origins. Am. J. Phys. Anthropol. 89, 29–58.
Gebo, D.L., Schwartz, G.T., 2006. Foot bones from Omo: Implications for hominid evolution. Am. J. Phys. Anthropol. 129, 499–511.
Gill, C.M., Taneja, A.K., Bredella, M.A., Torriani, M., DeSilva, J.M., 2014. Osteogenic relationship between the lateral plantar process and the peroneal tubercle in the human calcaneus. J. Anat. 224, 173–179.
Gómez-Olivencia, A., Quam, R., Sala, N., Bardey, M., Ohman, J.C., Balzeau, A., 2018. La Ferrassie 1: New perspectives on a "classic" Neandertal. J. Hum. Evol. 117, 13–32.
Greiner, T.M., Ball, K.A., 2014. Kinematics of primate midfoot flexibility. Am. J. Phys. Anthropol. 155, 610–620.
Griffin, N.L., D'Ao ût, K., Richmond, B., Gordon, A., Aerts, P., 2010. Comparative in vivo forefoot kinematics of *Homo sapiens* and *Pan paniscus*. J. Hum. Evol. 59, 608–619.
Grün, R., Stringer, C.B., 1991. Electron spin resonance dating and the evolution of modern humans. Archaeometry 33, 153–199.
Guérin, G., Frouin, M., Talamo, S., Aldeias, V., Bruxelles, L., Chiotti, L., Dibble, H.L., Goldberg, P., Hublin, J.J., Jain, M., Lahaye, C., Madelaine, S., Maureille, B., McPherron, S.J.P., Mercier, N., Murray, A.S., Sandgathe, D., Steele, T.E., Thomsen, K.J., Turq, A., 2015. A multi-method luminescence dating of the Palaeolithic sequence of La Ferrassie based on new excavations adjacent to the La Ferrassie 1 and 2 skeletons. J. Archaeol. Sci. 58, 147–166.
Gunz, P., Mitteroecker, P., Neubauer, S., Weber, G.W., Bookstein, F.L., 2009. Principles for the virtual reconstruction of hominin crania. J. Hum. Evol. 57, 48–62.
Gunz, P., Mitteroecker, P., 2013. Semilandmarks: A method for quantifying curves and surfaces. Hystrix 24, 103–109.
Harcourt-Smith, W.E.H., Aiello, L., 2004. Fossils, feet and the evolution of human bipedal locomotion. J. Anat. 204, 403–416.
Harcourt-Smith, W.H.E., Throckmorton, Z., Congdon, K.A., Zipfel, B., Deane, A.S., Drapeau, M.S.M., Churchill, S.E., Berger, L.R., Desilva, J.M., 2015. The foot of *Homo naledi*. Nat. Commun. 6, 1–8.
Harper, C.M., 2023. Human calcaneal variation relative to subsistence strategy, activity level, and footwear. Front. Earth Sci. 11, 1213374.
Harper, C.M., Ruff, C.B., Sylvester, A.D., 2021. Calcaneal shape variation in humans, nonhuman primates, and early hominins. J. Hum. Evol. 159, 103050.
Harper, C.M., Ruff, C.B., Sylvester, A.D., 2022a. Scaling and relative size of the human, nonhuman ape, and baboon calcaneus. Anat. Rec. 305, 100–122.
Harper, C.M., Zipfel, B., DeSilva, J.M., McNutt, E.J., Thackeray, F., Braga, J., 2022b. A new early hominin calcaneus from Kromdraai (South Africa). J. Anat. 241, 500–517.
Harvati, K., 2010. Neanderthals. Evo. Edu. Outreach 3, 367–376.
Hatala, K.G., Dingwall, H.L., Wunderlich, R.E., Richmond, B.G., 2013. Variation in foot strike patterns during running among habitually barefoot populations. PLoS One 8, e52548.
Heim, J.L., 1976. Les hommes fossiles de La Ferrassie. Tome I. Archives de l'Institut de Paléontologie Humaine, Mémoire 35. Masson, Paris.
Heim, J.L., 1982. Les hommes fossiles de La Ferrassie. Tome II: Les squelettes adultes (squelette des membres). Archives de l'Institut de Paléontologie Humaine, Mémoire 38. Masson, Paris.
Holloway, R.L., Yuan, M.S., Broadfield, D.C., 2005. Brain endocasts: The paleoneurological evidence. In: Schwartz, J., Tattersall, I. (Eds.), The Human Fossil Record Series. John Wiley & Sons, New York, pp. 209–270.
Holowka, N.B., Kraft, T.S., Wallace, I.J., Gurven, M., Venkataraman, V.V., 2022. Forest terrains influence walking kinematics among indigenous Tsimane of the Bolivian Amazon. Evol. Hum. Sci. 4, 1–17.
Holowka, N.B., Lieberman, D.E., 2018. Rethinking the evolution of the human foot: Insights from experimental research. J. Exp. Biol. 221, jeb174425.
Holowka, N.B., O'Neill, M.C., Thompson, N.E., Demes, B., Holowka, N.B., O'Neill, M.C., Thompson, N.E., Demes, B., 2017. Chimpanzee and human midfoot motion during bipedal walking and the evolution of the longitudinal arch of the foot. J. Hum. Evol. 104, 23–31.
Holowka, N.B., Wallace, I.J., Lieberman, D.E., 2018. Foot strength and stiffness are related to footwear use in a comparison of minimally- vs. conventionally-shod populations. Sci. Rep. 8, 1–13.
Holt, B.M., 2003. Mobility in Upper Paleolithic and Mesolithic Europe: Evidence from the lower limb. Am. J. Phys. Anthropol. 122, 200–215.
Holt, B.M., Formicola, V., 2008. Hunters of the Ice Age: The biology of Upper Paleolithic people. Am. J. Phys. Anthropol. 137, 70–99.
Koneru, M.C., Harper, C.M., 2024. Comparing lateral plantar process trabecular structure to other regions of the human calcaneus. Anat. Rec. 307, 3152–3165.
Latimer, B., Ohman, J.C., Lovejoy, C.O., 1987. Talocrural joint in African hominoids: Implications for *Australopithecus afarensis*. Am. J. Phys. Anthropol. 74, 155–175.
Latimer, B.M., Lovejoy, C.O., 1989. The calcaneus of *Australopithecus afarensis* and its implications for the evolution of bipedality. Am. J. Phys. Anthropol. 78, 369–386.
Lieberman, D.E., 2014. Strike type variation among Tarahumara Indians in minimal sandals versus conventional running shoes. J. Sport Health Sci. 3, 86–94.
Lockley, M., Roberts, G., Kim, J.Y., 2008. In the footprints of our ancestors: An overview of the hominid track record. Ichnos 15, 106–125.
López, N.R., Gómez, R.M., Valderrama, M.M., González, A.G., de la Torre-Montero, J.C., Moreno, Á.P.S., Fidalgo-Herrera, A.J., Ribeiro, A.S.F., López-Moreno, C., Martínez-Beltrán, M.J., 2023. Biomechanical analysis of barefoot walking and three different sports footwear in children aged between 4 and 6 years old. PLoS One 18, e0291056.
Lu, Z., Meldrum, D.J., Huang, Y., He, J., Sarmiento, E.E., 2011. The Jinniushan hominin pedal skeleton from the late Middle Pleistocene of China. Homo 62, 389–401.
Marchi, D., Rimoldi, A., García-Martínez, D., Bastir, M., 2022. Morphological correlates of distal fibular morphology with locomotion in great apes, humans, and *Australopithecus afarensis*. Am. J. Biol. Anthropol. 178, 286–300.
Mckeon, P.O., Hertel, J., Bramble, D., Davis, I., 2015. The foot core system: A new paradigm for understanding intrinsic foot muscle function. Br. J. Sports Med. 49, 290.
McNutt, E.J., Claxton, A.G., Carlson, K.J., 2017. Revisiting the peroneal trochlea of the StW 352 calcaneus. South Afr. J. Sci. 113, 1–5.
McNutt, E.J., Zipfel, B., DeSilva, J.M., 2018. The evolution of the human foot. Evol. Anthropol. 27, 197–217.
Moore, E.S., Kindig, M.W., McKearney, D.A., Telfer, S., Sangeorzan, B.J., Ledoux, W.R., 2019. Hind- and midfoot bone morphology varies with foot type and sex. J. Orthop. Res. 37, 744–759.
Mosca, V.S., 2010. Flexible flatfoot in children and adolescents. J. Child. Orthop. 4, 107–121.
Muñiz, F., Cáceres, L.M., Rodríguez-Vidal, J., Neto de Carvalho, C., Belo, J., Finlayson, C., Finlayson, G., Finlayson, S., Izquierdo, T., Abad, M., Jiménez-Espejo, F.J., Sugisaki, S., Gómez, P., Ruiz, F., 2019. Following the last Neanderthals: Mammal tracks in Late Pleistocene coastal dunes of Gibraltar (S Iberian Peninsula). Quatern. Sci. Rev. 217, 297–309.
Neto de Carvalho, C., Proença Cunha, P., Belo, J., Muñiz, F., Baucon, A., Cachão, M., Figueiredo, S., Buylaert, J.-P., Galán, J.M., Belaústegui, Z., et al., 2025. Neanderthal coasteering and the first Portuguese hominin tracksites. Sci. Rep. 15, 23785.
Nozaki, S., Watanabe, K., Kamiya, T., Katayose, M., Ogihara, N., 2020. Three-dimensional morphological variations of the human calcaneus investigated using geometric morphometrics. Clin. Anat. 33, 751–758.
Nozaki, S., Amano, H., Oishi, M., Ogihara, N., 2021. Morphological differences in the calcaneus among extant great apes investigated by three-dimensional geometric morphometrics. Sci. Rep. 11, 20889.
O'Neill, M.C., Demes, B., Thompson, N.E., Umberger, B.R., 2018. Three-dimensional kinematics and the origin of the hominin walking stride. J. R. Soc. Interface 15, 20180205.
Pablos, A., 2015. The foot in the Homo fossil record. Mitteilungen der Gesellschaft für Urgeschichte 24, 11–28.
Pablos, A., Arsuaga, J.L., 2024. Tarsals from the Sima de los Huesos Middle Pleistocene site (Atapuerca, Burgos, Spain). Anat. Rec. 307, 2635–2664.
Pablos, A., Gómez-Olivencia, A., Maureille, B., Holliday, T.W., Madelaine, S., Trinkaus, E., Couture-Veschambre, C., 2019. Neandertal foot remains from Regourdou 1 (Montignac-sur-Vézère, Dordogne, France). J. Hum. Evol. 128, 17–44.
Pablos, A., Martínez, I., Lorenzo, C., Sala, N., Gracia-Téllez, A., Arsuaga, J.L., 2014. Human calcanei from the Middle Pleistocene site of Sima de los Huesos (Sierra de Atapuerca, Burgos, Spain). J. Hum. Evol. 76, 63–76.
Pablos, A., Pantoja-Pérez, A., Martínez, I., Lorenzo, C., Arsuaga, J.L., 2017. Metric and morphological analysis of the foot in the Middle Pleistocene sample of Sima de los Huesos (Sierra de Atapuerca, Burgos, Spain). Quatern. Int. 433, 103–113.
Pearson, O.M., 2000. Activity, climate, and postcranial robusticity. Curr. Anthropol. 41, 569–607.
Pearson, O.M., Cordero, R.M., Busby, A.M., 2006. How different were Neanderthals' habitual activities? A comparative analysis with diverse groups of recent humans. In: Harvati, Katerina, Harrison, T. (Eds.), Neanderthals Revisited: New Approaches and Perspectives Edited by Katerina Harvati. Springer, Dordrecht., pp. 135–156
Pearson, O.M., Pablos, A., Rak, Y., Hovers, E., 2020. A partial Neandertal foot from the Late Middle Paleolithic of Amud cave, Israel. PaleoAnthropology 98–125.
Pietrobelli, A., Sorrentino, R., Benazzi, S., Belcastro, M.G., Marchi, D., 2024a. Linking the proximal tibiofibular joint to hominid locomotion: A morphometric study of extant species. Am. J. Biol. Anthropol. 184, e24696.
Pietrobelli, A., Sorrentino, R., Notariale, V., Durante, S., Benazzi, S., Marchi, D., Belcastro, M.G., 2022. Comparability of skeletal fibulae surfaces generated by different source scanning (dual-energy CT scan vs. high resolution laser scanning) and 3D geometric morphometric validation. J. Anat. 241, 667–682.
Pietrobelli, A., Sorrentino, R., Sparacello, V.S., Mottes, E., Fontana, F., Sineo, L., Benazzi, S., Marchi, D., Belcastro, M.G., 2024b. Exploring the role of fibular extremities as indicators of mobility patterns and locomotor behavior in *Homo sapiens* from Mid-Late Upper Paleolithic to the modern age. Archaeol. Anthropol. Sci. 16, 100.
Prang, T.C., 2015a. Calcaneal robusticity in Plio-Pleistocene hominins: Implications for locomotor diversity and phylogeny. J. Hum. Evol. 80, 135–146.

Prang, T.C., 2015b. Rearfoot posture of *Australopithecus sediba* and the evolution of the hominin longitudinal arch. Sci. Rep. 5, 17677.
Prang, T.C., 2016. The subtalar joint complex of *Australopithecus sediba*. J. Hum. Evol. 90, 105–119.
Prang, T.C., 2024. The relative size of the calcaneal tuber reflects heel strike plantigrady in African apes and humans. Am. J. Biol. Anthropol. 183, e24865.
Raichlen, D.A., Armstrong, H., Lieberman, D.E., 2011. Calcaneus length determines running economy: Implications for endurance running performance in modern humans and Neandertals. J. Hum. Evol. 60, 299–308.
Rosas, A., Ferrando, A., Bastir, M., García-Tabernero, A., Estalrrich, A., Huguet, R., García-Martínez, D., Pastor, J.F., de la Rasilla, M., 2017. Neandertal talus bones from El Sidrón site (Asturias, Spain): A 3D geometric morphometrics analysis. Am. J. Phys. Anthropol. 164, 394–415.
Rosas, A., Martínez-Maza, C., Bastir, M., García-Tabernero, A., Lalueza-Fox, C., Huguet, R., Eugenio Ortiz, J., Julià, R., Soler, V., de Torres, T., Martínez, E., Carlos Cañ averas, J., Sá nchez-Moral, S., Cuezva, S., Lario, J., Santamaría, D., de la Rasilla, M., Fortea, J., 2006. Paleobiology and comparative morphology of a late Neandertal sample from El Sidrón, Asturias, Spain. Proc. Natl. Acad. Sci. 103, 19266–19271.
Ryan, T.M., Shaw, C.N., 2015. Gracility of the modern *Homo sapiens* skeleton is the result of decreased biomechanical loading. Proc. Natl. Acad. Sci. 112, 372–377.
Saers, J.P.P., Ryan, T.M., Stock, J.T., Saers, Jaap P.P., Ryan, Timothy M., Stock, J.T., 2018. Trabecular bone functional adaptation and sexual dimorphism in the human foot. Am. J. Phys. Anthropol. 168, 154–169.
Semal, P., Crevecoeur, I., Flas, D., Hauzeur, A., Maureille, B., Germonpre, M., Cammaert, L., Clerck, N. De, Hambucken, A., Higham, T., Toussaint, M., Plicht, J. Van Der, 2009. New data on the late Neandertals: Direct dating of the Belgian Spy fossils. Am. J. Phys. Anthropol. 138, 421–428.
Shaw, C.N., Stock, J.T., 2011. The influence of body proportions on femoral and tibial midshaft shape in hunter-gatherers. Am. J. Phys. Anthropol. 144, 22–29.
Sineo, L., Bigazzi, R., D'Amore, G., Tartarelli, G., Di Patti, C., Berzero, A., Caramella Crespi, V., 2002. I resti umani della Grotta di S. Teodoro (Messina): Datazione assoluta con il metodo della spettrometria gamma diretta (U/Pa). Antropo 2, 9–16.
Slice, D.E., 2006. Modern Morphometrics in Physical Anthropology. Springer Science & Business Media.
Sorrentino, R., Carlson, K.J., Bortolini, E., Minghetti, C., Feletti, F., Fiorenza, L., Frost, S., Jashashvili, T., Parr, W., Shaw, C., Su, A., Turley, K., Wroe, S., Ryan, T.M., Belcastro, M.G., Benazzi, S., 2020a. Morphometric analysis of the hominin talus: Evolutionary and functional implications. J. Hum. Evol. 142, 102747.
Sorrentino, R., Carlson, K.J., Figus, C., Pietrobelli, A., Stephens, N.B., DeMars, L.J.D., Saers, J.P.P., Armando, J., Bettuzzi, M., Guarnieri, T., Oxilia, G., Vazzana, A., Parr, W., Turley, K., Morigi, M.P., Stock, J.T., Ryan, T.M., Benazzi, S., Marchi, D., Belcastro, M.G., 2022. The talar morphology of a hypochondroplasic dwarf: A case study from the Italian Late Antique period. Int. J. Osteoarchaeol. 32, 429–443.
Sorrentino, R., Carlson, K.J., Orr, C.M., Pietrobelli, A., Figus, C., Li, S., Conconi, M., Sancisi, N., Belvedere, C., Zhu, M., Fiorenza, L., Hublin, J.J., Jashashvili, T., Novak, M., Patel, B.A., Prang, T.C., Williams, S.A., Saers, J.P.P., Stock, J.T., Ryan, T., Myerson, M., Leardini, A., DeSilva, J., Marchi, D., Belcastro, M.G., Benazzi, S., 2023. Morphological and evolutionary insights into the keystone element of the human foot's medial longitudinal arch. Commun. Biol. 6, 1061.
Sorrentino, R., Pietrobelli, A., Mameli, D., Mariotti, V., Nicolosi, T., Belcastro, M.G., 2025. The virtual database of the documented human osteological collection (DHOC) of the Certosa Cemetery of Bologna (Italy, 19th-20th Century). Am. J. Biol. Anthropol. 186, e25065.
Sorrentino, R., Stephens, N.B., Carlson, K.J., Figus, C., Fiorenza, L., Frost, S., Harcourt-Smith, W., Parr, W., Saers, J., Turley, K., Wroe, S., Belcastro, M.G., Ryan, T.M., Benazzi, S., 2020b. The influence of mobility strategy on the modern human talus. Am. J. Phys. Anthropol. 171, 456–469.
Sorrentino, R., Stephens, N.B., Marchi, D., DeMars, L.J.D., Figus, C., Bortolini, E., Badino, F., Saers, J.P.P., Bettuzzi, M., Boschin, F., Capecchi, G., Feletti, F., Guarnieri, T., May, H., Morigi, M.P., Parr, W., Ricci, S., Ronchitelli, A., Stock, J.T., Carlson, K.J., Ryan, T.M., Belcastro, M.G., Benazzi, S., 2021. Unique foot posture in Neanderthals reflects their body mass and high mechanical stress. J. Hum. Evol. 161, 103093.
Sparacello, V.S., Dori, I., Rossi, S., Varalli, A., Riel-Salvatore, J., Gravel-Miguel, C., Riga, A., Seghi, F., Goude, G., Palstra, S.W.L., Starnini, E., Formicola, V., Moggi-Cecchi, J., 2021. New human remains from the Late Epigravettian necropolis of Arene Candide (Liguria, northwestern Italy): Direct radiocarbon evidence and inferences on the funerary use of the cave during the Younger Dryas. Quatern. Sci. Rev. 268, 107131.
Sparacello, V.S., Rossi, S., Pettitt, P., Roberts, C.A., Salvatore, J.R., Formicola, V., 2018a. New insights on Final Epigravettian funerary behaviour at Arene Candide Cave (Western Liguria, Italy) from osteological and spatial analysis of secondary bone deposits. J. Anthropol. Sci. 96, 161–184.
Sparacello, V.S., Villotte, S., Shaw, C.N., Fontana, F., Mottes, E., Starnini, E., Dalmeri, G., Marchi, D., 2018b. Changing mobility patterns at the Pleistocene-Holocene transition. Lower limb biomechanics of Italian Gravettian and Mesolithic individuals. In: Palaeolithic Italy. Advanced Studies on Early Human Adaptation in the Apennine Peninsula. Sidestone Press, pp. 357–396.
Stern, J.T., Susman, R.L., 1983. The locomotor anatomy of *Australopithecus afarensis*. Am. J. Phys. Anthropol. 60, 279–317.
Su, A., Carlson, K.J., 2017. Comparative analysis of trabecular bone structure and orientation in South African hominin tali. J. Hum. Evol. 106, 1–18.
Tomizawa, Y., Nakatsukasa, M., Ponce de León, M.S., Zollikofer, C.P.E., Morimoto, N., 2024. Shaft structure of the first metatarsal contains a strong phylogenetic signal in apes and humans. Am. J. Biol. Anthropol. 185, e24987.
Treherne, P., Lee, E.C.S., Rainbow, M.J., Kelly, L.A., 2025. Mitigating stress: Exploring how our feet change shape with size. R. Soc. Open Sci. 12, 241828.
Trinkaus, E., 1975. Squatting among the neandertals: A problem in the behavioral interpretation of skeletal morphology. J. Archaeol. Sci. 2, 327–351.
Trinkaus, E., 1983. Functional aspects of Neandertal pedal remains. Foot Ankle 3, 377–390.
Trinkaus, E., 2005. Anatomical evidence for the antiquity of human footwear use. J. Archaeol. Sci. 32, 1515–1526.
Trinkaus, E., Churchill, S.E., Villemur, I., Riley, K.G., Heller, J.A., Ruff, C.B., 1991. Robusticity versus shape: The functional interpretation of Neandertal appendicular morphology. J. Anthropol. Soc. Nippon 99, 257–278.
Trudeau, M.B., Jewell, C., Rohr, E., Fischer, K.M., Willwacher, S., Brueggemann, G.P., Hamill, J., 2017. The calcaneus adducts more than the shoe's heel during running. Footwear Sci. 9, 79–85.
Tsegai, Z.J., Skinner, M.M., Gee, A.H., Pahr, D.H., Treece, G.M., Hublin, J., Kivell, T.L., 2017. Trabecular and cortical bone structure of the talus and distal tibia in *Pan* and *Homo*. Am. J. Phys. Anthropol. 163, 784–805.
Tsegai, Z.J., Skinner, M.M., Pahr, D.H., Hublin, J.J., Kivell, T.L., 2018. Systemic patterns of trabecular bone across the human and chimpanzee skeleton. J. Anat. 232, 641–656.
Vandermeersch, B., Bar-Yosef, O., 2019. The Paleolithic Burials at Qafzeh Cave, Israel. Paléo 30-1, 256–275.
Vandermeersch, B., 1981. Les hommes fossiles de Qafzeh (Israël). Éditions du CNRS, Paris.
Wagner, U.A., Sangeorzan, B.J., Harrington, R.M., Tencer, A.F., 1992. Contact characteristics of the subtalar joint: Load distribution between the anterior and posterior facets. J. Orthop. Res. 10, 535–543.
Wallace, I.J., Koch, E., Holowka, N.B., Lieberman, D.E., 2018. Heel impact forces during barefoot versus minimally shod walking among tarahumara subsistence farmers and urban Americans. R. Soc. Open Sci. 5, 180044.
Weaver, T.D., Steudel-numbers, K., 2005. Does climate or mobility explain the differences in body proportions between Neandertals and their Upper Paleolithic successors? Evol. Anthropol. 14, 218.
Webber, J.T., Raichlen, D.A., 2016. The role of plantigrady and heel-strike in the mechanics and energetics of human walking with implications for the evolution of the human foot. J. Exp. Biol. 219, 3729–3737.
Willems, C., Stassijns, G., Cornelis, W., D'Août, K., 2017. Biomechanical implications of walking with indigenous footwear. Am. J. Phys. Anthropol. 162, 782–793.
Wood, R.E., Higham, T.F.G., De Torres, T., Tisnérat-Laborde, N., Valladas, H., Ortiz, J.E., Lalueza-Fox, C., Sánchez-Moral, S., Cañaveras, J.C., Rosas, A., 2013. A new date for the Neanderthals from El Sidrón Cave (Asturias, northern Spain). Archaeometry 55, 148–158.
Zeininger, A., Patel, B.A., Zipfel, B., Carlson, K.J., 2016. Trabecular architecture in the StW 352 fossil hominin calcaneus. J. Hum. Evol. 97, 145–158.
Zeininger, A., Schmitt, D., Wunderlich, R.E., 2020. Mechanics of heel-strike plantigrady in African apes. J. Hum. Evol. 145, 102840.
Zipfel, B., Berger, L.R., 2007. Shod versus unshod: The emergence of forefoot pathology in modern humans? Foot 17, 205–213.
Zipfel, B., DeSilva, J.M., Kidd, R.S., Carlson, K.J., Churchill, S.E., Berger, L.R., 2011. The foot and ankle of *Australopithecus sediba*. Science 333, 1417–1420.